Sequence stratigraphic reconstruction of the late Middle Devonian Geneseo Formation of NY, USA: Developing a genetic model for "Upper Devonian" unconventional targets in the Northern Appalachian Basin

Ryan D. Wilson [a,*,1], Juergen Schieber [a], Kevin M. Bohacs [b]

[a] Department of Geological Sciences, Indiana University, Bloomington, IN, USA
[b] KMBohacs GEOconsulting, Houston, TX, USA

ABSTRACT

The late Middle Devonian Geneseo Formation and its lateral equivalents in the northern Appalachian Basin are significant secondary targets to the extensively explored Marcellus Sub-group. Surface to sub-surface characterization of the mudstone-dominated Geneseo Formation combines detailed observations of facies, facies associations, stratal architecture, stratal geometry, and stratal terminations, in combination with geochemical proxies to assess proximal to distal trends and enable prediction of hydrocarbon play element quality and distribution. Correlations within this mudstone-rich succession are conducted at the parasequence-scale, and incorporate detailed descriptions of four drill cores, >100 outcrops, and mapping of >500 wireline logs.

The Geneseo Formation herein has been subdivided into two depositional sequences comprising three lithostratigraphic units (i.e., Lower Geneseo, Fir Tree, and Upper Geneseo members respectively). The Lower and Upper Geneseo members show systematic aggradational to progradational parasequence stacking patterns, as well as downlap–onlap stratal terminations with underlying strata; these members represent highstand systems tracts. The Fir Tree Member occurs between the Lower and Upper Geneseo members, truncates the underlying Lower Geneseo, shows progradational–aggradational–retrogradational parasequence stacking patterns, and spans two systems tracts: lowstand and transgressive.

Isopach maps were constructed within the high-resolution sequence-stratigraphic framework to better understand thickness trends at the landing-zone scale. Thickness variation across the basin suggests reactivation of basement structures and syndepositional faulting strongly influenced accommodation. Specifically, the N–S trending Clarendon-Linden Fault System appears to have been a western sediment barrier during Geneseo time and the primary depocenter of fine-grained clastics occurs in south-central NY in a structural low. As the Geneseo system advanced, the succession sequentially filled topographic lows from east to west (proximal to distal). Understanding the controls on reservoir quality and distribution of secondary and tertiary targets to the Marcellus can facilitate ranking and prioritization of landing-zones, as well as optimization of well placement for completion design.

1. Introduction

The late Middle Devonian (Givetian) Geneseo Formation and correlative units (i.e., Burket Shale) are considered key secondary targets for the Marcellus Sub-group throughout the Appalachian Basin. Although there is significant economic potential for this unconventional target, the lack of data and detailed geologic characterization of the Geneseo/Burket succession hinder the ability to assess hydrocarbon potential (i.e., EUR) and spatial distribution of hydrocarbon play elements. As a result, analog data from the underlying Marcellus Sub-group are typically applied to "Upper Devonian" targets, even though such targets may represent different depositional environments, organic matter quality and richness, distribution of fracture barriers/baffles, as well as other reservoir properties (i.e., saturation, composition, mechanical properties). Thus, the use of Marcellus reservoir properties and cutoffs for "Upper Devonian" targets may introduce significant uncertainty during exploration.

Key controls on unconventional reservoir quality and distribution in fine-grained, mudstone-dominated successions include total organic carbon (TOC), organic matter type (e.g., Type I-II liquid prone, Mixed Type II/III, or type III gas prone), mineralogy (i.e., clay content/ductility, brittleness, "fracability"), presence and distribution of high-strength rocks (i.e., fracture barriers/baffles), thermal maturity (0.8–1.3 for liquids-rich play), porosity/permeability, presence and distribution of natural fractures, and thickness of pay interval (Bohacs et al., 2005, 2012; Gale et al., 2014; Passey et al., 2010; Wilson and Schieber, 2016; Wilson et al., 2020; Katz et al., 2021; Venieri et al., 2021).

* Corresponding author.
  URL: http://ryanwilson@chevron.com (R.D. Wilson).
[1] Present Address: Chevron Technology Center, Houston, TX, U.S.A

Unconventional resources show characteristically low permeabilities, which is directly a result of textural attributes and composition (particle diameter <62.5 μm), diagenetic alteration (i.e., secondary precipitation of void-filling clays and cements), as well as small-scale vertical and lateral heterogeneity (i.e., bedding styles and continuity, facies change, geobody distribution, diagenetic alteration or emplacement). Therefore, it is necessary to employ fundamental sedimentologic and stratigraphic workflows in combination with organic and inorganic geochemical data to develop a robust geologic model for prediction of hydrocarbon play elements at an exploration-scale (regional), as well as play element variation at the well-pad scale (landing-zone variation). Through surface and sub-surface characterization, data and interpretations regarding stratigraphic architecture, lithofacies variation, compositional trends, and total organic content can be evaluated and mapped to develop a fully integrated sequence stratigraphic model (Bohacs et al., 2005). Furthermore, proximal–distal relations within the geologic system can be better understood for identifying distribution and richness of potential target zones for exploration and development.

This study explores the genetic relations in what has been interpreted as an epicontinental basin that was persistently dysoxic, high-productivity, and shallow-water (10's of meters water depth) wherein organic-rich, fine-grained clastics were deposited and transported laterally for 100's of kilometers through a variety of depositional processes (Wilson and Schieber, 2014, 2015, 2017a; Lash, 2016; Smith et al., 2019; Li et al., 2020). Moreover, sedimentary environments and facies distribution at the parasequence-scale were evaluated temporally and spatially to illustrate the dominant controls on source rock development and reservoir quality throughout the basin. This high-resolution sequence stratigraphic framework incorporates surface (i.e., outcrops) and sub-surface (i.e., drill cores, wireline logs) data throughout New York state, and represents a basin-scale assessment of a dominantly progradational muddy prodeltaic system that accumulated during a major orogenic event (Acadian Orogeny, 3rd Tectophase; Ettensohn, 1985) as well as a eustatic rise (Johnson, 1970; Johnson et al., 1985). The combination of sub-surface mapping, outcrop and core description, thin-section petrography and scanning electron microscopy (SEM), with organic- and inorganic-geochemical characterization facilitated the recognition and predictability of optimal hydrocarbon source and unconventional targets throughout the basin. In addition, combination of these data enabled the development of a robust geologic model for "Upper Devonian" targets of the northern Appalachian Basin (NAB). Furthermore, providing a framework to better understand thickness changes throughout the basin, as well as depositional limits that have resulted in a paradigm shift for deposition of organic-rich shales in the Appalachian Basin (Smith et al., 2019). This study details at the parasequence-scale genetic relations in sedimentary facies, depositional environment, paleoecological interpretations, as well as reservoir quality and presence that are strongly impacted by pre-existing basement structures.

Through applying fundamental sequence-stratigraphic principles, sedimentary successions can be differentiated into a chronostratigraphic framework based upon stratal architecture, stratal geometries, stratal terminations, stacking patterns, and facies and facies associations (Van Wagoner et al., 1988; Abreu et al., 2010). Once a genetic framework is developed, inferences regarding sediment delivery, accommodation, and shoreline trajectory enables prediction away from data control (Bohacs et al., 2005; Donovan and Staerker, 2010). Through the development of a fully integrated sequence-stratigraphic framework and incorporation of surface and subsurface data, hydrocarbon play element quality and distribution can be evaluated, which is critical for economic success.

Throughout the exploration of Middle and Late Devonian targets, vertical and lateral variability in thickness, mechanical properties, and organic content was not adequately explained with pre-existing depositional models that view these deposits as the result of continuous slow sediment accumulation through suspension settling of clay and silt in a stratified water column with persistently anoxic conditions throughout the basin (Baird and Brett, 1991; Formolo and Lyons, 2007). Motivation to reassess variance in rock properties is a result of the encountered spatial and temporal trends in production in these targets (Initial production ranges from 4 to 8 MMscf/d, can be over 20 MMscf/d under consistent completion design, thermal maturity, and pressure (Agbaji et al., 2009; Ejofodomi et al., 2011)).

At closer inspection of these Devonian organic-matter-rich units, an array of sedimentary features suggests multiple modes of sediment transport and deposition in a dynamic river-flood-influenced, storm-wave-dominated depositional environment (Wilson and Schieber, 2014, 2015, 2017a; Smith et al., 2019). These features include scour surfaces, terrestrial phytodetritus, normal and inverse lamina-set grading, current- and wave-formed features, soft-sediment deformation, as well as varying intensity and diversity of bioturbation. The variability preserved in these strata, although at times quite subtle and cryptic, requires a detailed sedimentologic and petrographic evaluation from the macro-to nano-scale to conduct an integrated reservoir characterization (Bohacs et al., 2012; Lazar et al., 2015; Schieber et al., 2016; Wilson and Schieber, 2016; Wilson et al., 2020).

2. Geologic setting

There is a long history of geological study in the Devonian foreland strata of the NAB, representing a global reference section due to the nearly complete stratigraphic record with significant continuous sections exposed throughout the state (Hall, 1843; Kindle, 1896; Ulrich, 1911; Grabau, 1913). During Devonian time, oblique convergence between Laurentia and Avalon terranes fostered magmatic arc volcanism and formation of a retroarc fold and thrust belt (i.e., Hudson Valley Fold and Thrust Belt) that loaded the eastern edge of the North American craton (Ettensohn, 1985, 1987) (Fig. 1). This event drastically reshaped the structural makeup of the basin, which is preserved in the sedimentary record as an abrupt transition from widespread platform carbonate deposition (i.e., Tully Limestone) into distal offshore organic-matter-rich fine-grained clastics (i.e., Geneseo/Burket black shales; Fig. 2). Moreover, this collisional event appears to have had a dramatic effect on reactivating preexisting structural elements throughout the basin (Fig. 3), in particular the N–S oriented Clarendon–Lindon fault system (Chadwick, 1920; Van Tyne, 1975; Jacobi and Fountain, 2002).

Cratonic downwarping and subsidence of the Appalachian Basin was compounded with a eustatic rise (that generated the well-known Taghanic Onlap; Johnson, 1970), resulting in regional inundation of the craton with a broad, persistently dysoxic epicontinental seaway. At time of deposition, the NAB was situated 30–35° south of the equator (Fig. 1). Portions of Laurentia were emergent while other portions were covered by a shallow sea (Fig. 1). Globally, the Middle–Late Devonian has been characterized to have been dominated by a warm climate mode (Frakes et al., 1992) with 4–12 times present day pCO_2 (Berner, 1990). Environmental conditions for the NAB at this time were seasonally variable and arid to semiarid (Woodrow, 1985; Witzke and Heckel, 1988), and thus this region should have been extensively affected by tropical storms, a perspective that is supported by evidence for storm-influenced sedimentation throughout the NAB, such as widespread tempestites and erosional contacts (Miller et al., 1988; Schieber, 1994, 1998; Brett et al., 2003).

Changing basinal conditions along with potential global warming and sea-level changes may have significantly contributed to what is referred to as the global Taghanic Bioevent, which resulted in the demise of Middle Devonian taxa worldwide and impactful shifts in trophic and community structure (Johnson, 1970; Aboussalam, 2003; Baird and Brett, 2008; Zambito et al., 2012). As the hinterland was carved and denuded, enhanced delivery of fine-grained detritus and terrestrial-derived nutrients fostered high surface water algal productivity and widespread burial of organic carbon (Algeo et al., 1995). The
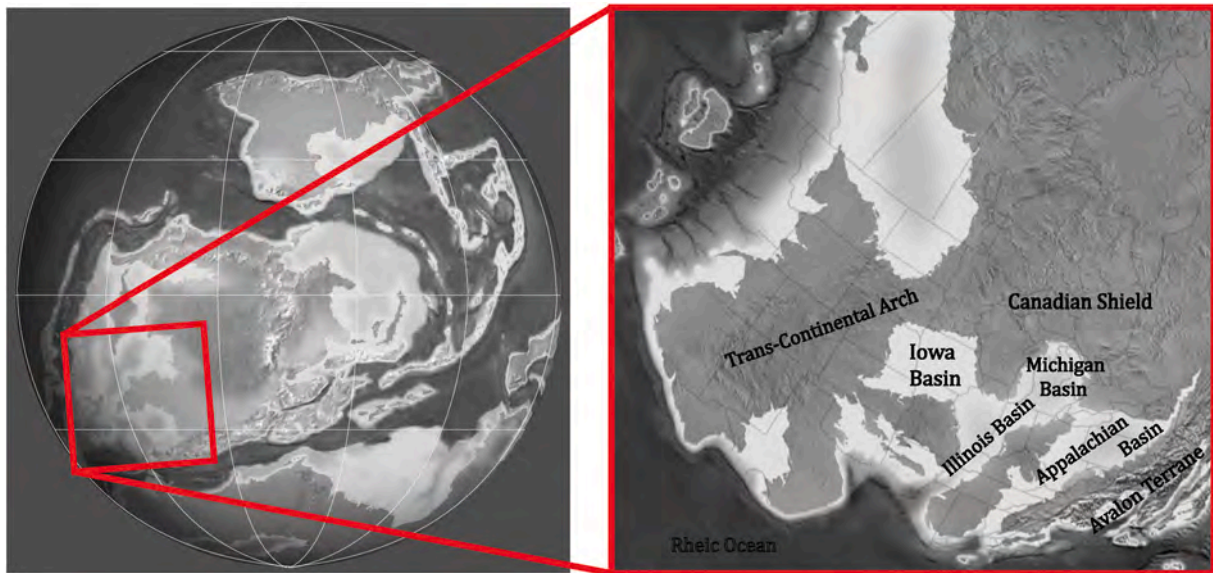
Fig. 1. Middle Devonian Paleogeographic map modified after Blakey (2005). Global map zooms into eastern North America (i.e., Laurentia) during the oblique convergence with a series of microcontinents. This collision produced a scissor-like closure and uplift of the Avalon Terrane which supplied sediments to the Appalachian Basin.
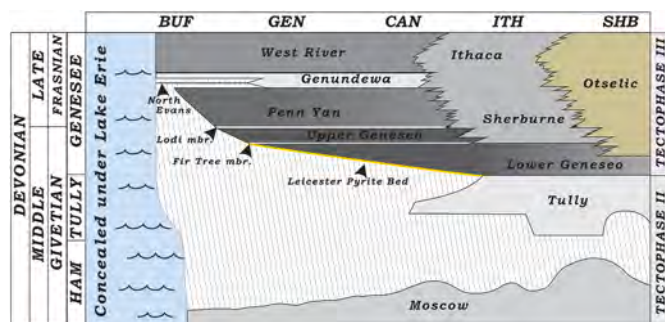
Fig. 2. Generalized chronostratigraphic chart for Middle–Late Devonian strata of New York (SHB, Sherburne; ITH, Ithaca; CAN, Canandaigua; GEN, Geneseo; BUF, Buffalo; HAM, Hamilton Group). The Geneseo Formation marks the onset of the third tectophase of the Acadian Orogeny, the most pronounced thrust loading event of that orogeny. The Genesee Group onlaps the Taghanic disconformity westward; thus, the basal ages of the onlapping Geneseo and Penn Yan shales become progressively younger westward (Wilson and Schieber, 2015).

Devonian Period was marked by many changes in marine and terrestrial ecosystems, most notably the proliferation of vascular plants that led to enhanced weathering and nutrient flux to the oceans (Algeo et al., 1995), and likely enabled globally extensive deposition of organic-matter-rich black mudstones. Although both phytoplankton and land plants preferentially incorporate ^{12}C into their biomass during photosynthesis, land plants use stomata to regulate gas exchange with the atmosphere, and thus are not as influenced by ambient CO_2 concentration as are marine photoautotrophs. The isotopic consequences of this effect allow the differentiation of marine vs terrestrial organic matter input (Maynard, 1981; Wilson and Schieber, 2017b), and are further enhanced during periods of high atmospheric pCO_2 (Arthur et al., 1988).

Drainage of the Acadian terrain fueled delta growth and extensive offshore delivery of fine-grained clastics which is expressed as aggradational to progradational stacking patterns observed in the Geneseo Formation (Wilson and Schieber, 2017a). Peak of organic-carbon preservation is recognized in basal parasequences of the Geneseo Formation, with preferential enrichment of the unit westward from the Catskill delta. Following active thrust loading, sediment input eventually outcompeted the rate of basin subsidence and the foreland basin filled with clastic sediments. The succession consists of a multitude of mudstone facies that can be grouped into different facies associations and differentiated into genetically-related packages based on their stratal geometry and parasequence development through the use of physical, biologic, and chemical attributes.

3. Methods

The current investigation relies on surface exposures (~100), drill cores (4), and wireline logs (519) throughout the entire state of New York (Fig. 4). Outcrop exposures were visited on multiple occasions for photomosaics, detailed descriptions, and sampling which for many locations required excavation to reveal fresh material. Outcrops also provide key sources for biostratigraphic sub-divisions in previous studies that facilitated surface to sub-surface correlations of genetic framework (Baird et al., 1988; House and Kirchgasser, 1993). Detailed lithologic profiles were recorded at each locality and samples stabilized with epoxy resin and thin-sectioned (thickness 20–25 mm). Hand specimens were slabbed with a rock saw and then smoothed and polished with grinding wheels of successively finer grit sizes (60–1200). High-resolution images of polished slabs and thin sections were acquired by digital photography and with a flatbed scanner (1200–2400 dpi resolution).

Observations of texture, sedimentary features, bioturbation index, ichnogenera, diagenetic overprint, and bed thickness, shape, and continuity were recorded at outcrops as well as at drill core locations. Drill core preserve more depositional textures due to the lack of exposure to weathering, whereas outcrops facilitate the characterization of 3-dimensional stratigraphic architecture, stacking patterns, stratal terminations and key surfaces, as well as bedset-scale relations and trends. Moreover, surface exposures aid the inquiry of depositional processes and systematic characterization of transport mechanisms, especially in the context of flow evolution and lateral variability of depositional elements. Through variable lighting, as well as wet vs. dry imaging, detailed image sets of sedimentary features at the hand specimen scale were acquired.

Thin sections (>200) were used to examine microfacies variation, small-scale sedimentary features (lamina truncations, graded beds,
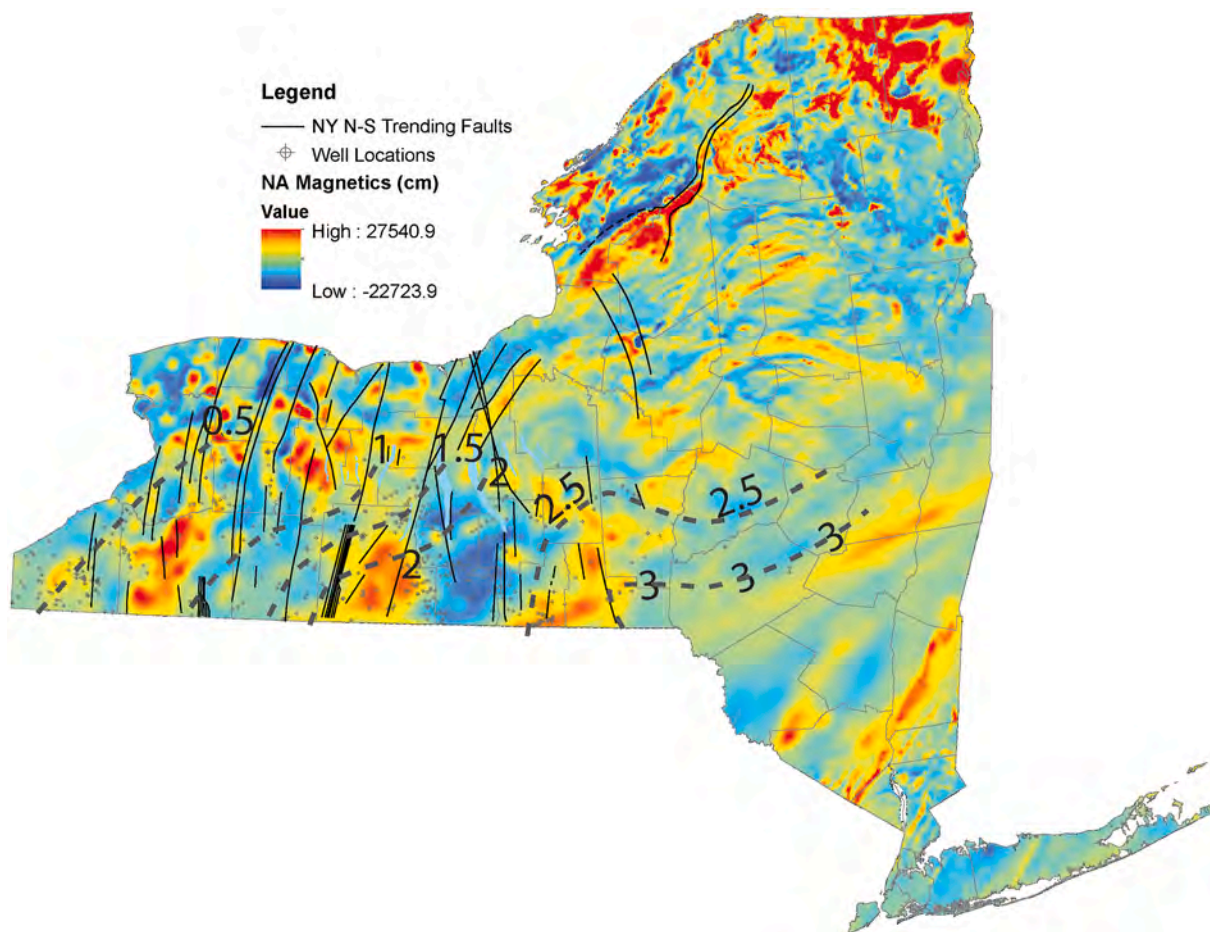
Fig. 3. A) Map of magnetics. Magnetics from the Ohio Geological Survey and United States Geological Survey (Zietz, 1982). Red is high, blue is low. In addition, vitrinite reflectance contours outline thermal maturity trends in the Devonian section, ranging from dry gas to the east to early oil window to the west (Weary et al., 2000; Smith and Leone, 2010). (For interpretation of the references to colour in this figure legend, the reader is referred to the Web version of this article.)
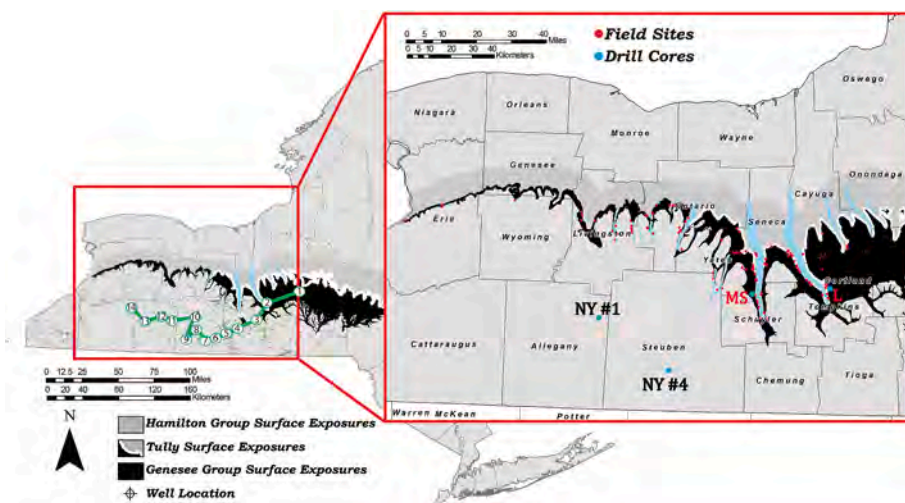
Fig. 4. Overview map of New York and locations of outcrops and drill cores (L = Lansing Core, MS = Morton Salt Core, NY#1/#4 core). Wells in green included in Fig. 5 section. (For interpretation of the references to colour in this figure legend, the reader is referred to the Web version of this article.)

stratification styles, etc.), compositional and textural changes, and bioturbation styles. The bioturbation index (BI) of Taylor and Goldring (1993) was used to quantify bioturbation intensity. Drill-core, hand-specimen, and thin-section descriptions were combined to comprehensively evaluate centimeter-to decimeter-scale heterogeneity, lithofacies,

and stratal architecture. Thin-sections were also used in SEM analysis for cursory assessment of depositional fabric, however, ion milled sections were the primary approach for fabric analysis using an FEI Quanta 400 FEG SEM. For ion mill preparation, 5 × 5 mm slices were mounted and ion milled using the Gatan 600 DuoMill™ for to produce smooth and

mechanically unaltered surfaces for analyzing pores and grains in the nanometer-size range. The possibility that artificial pores might be produced in organic-matter (OM) due to ion-beam heating was a serious concern. We adopted the procedure outlined in Wilson and Schieber (2016) to eliminate misinterpretation of artifacts, which has subsequently been validated to produce a nearly flat surface for analyzing pore structure without creating artificial pores (Mastalerz and Schieber, 2017).

For geochemical analyses, samples were selected from drill core at 40-cm intervals. Samples were ground with a SPEX 8000 ball mill with a steel vial for 10–15 min, weighed into a polyethylene centrifuge tube (~1 g), and subsequently acidified for 24 h with 1N hydrochloric acid (HCl). Subsequently samples were centrifuged for 10 min and the supernatant was drained. De-ionized water was added and mixed with each sample and centrifuged three times to remove remaining HCl from the ground sample. Samples were subsequently frozen, and freeze-dried to remove liquids. The samples were then weighed into tin capsules (~0.30 μg), placed into the autosampler of the elemental analyzer and combusted. Stable isotope ratios of organic carbon ($\delta^{13}C_{org}$) were determined using a ThermoFinnigan Delta Plus XP mass-spectrometer connected to a Costech Elemental Analyzer. The carbon isotopic composition of the resulting CO_2 gas was measured against internal laboratory standards (e.g., acetanilide, $\delta_{13}C_{org} = -29.85‰$) that had been calibrated with the Vienna Peedee Belemnite (VPDB) isotopic standard. Total carbon and sulfur were determined with a C–S Eltra Analyzer on powdered samples. For X-ray fluorescence (XRF), outcrop and drill core samples were slabbed and polished to produce nearly flat surface topography, and then analyzed with an ITRAX core scanner at 4-mm resolution at the Large Lakes Observatory in Duluth, Minnesota.

Through applying fundamental sequence-stratigraphic principles, sedimentary successions can be differentiated into a chronostratigraphic framework based upon stratal architecture, stratal geometries, stratal terminations, stacking patterns, and facies and facies associations (Van Wagoner, 1977; Abreu et al., 2010). Once a genetic framework is developed, inferences regarding sediment delivery, accommodation, and shoreline trajectory enables prediction away from data control (Bohacs et al., 2005; Donovan and Staerker, 2010). Through the development of a fully integrated sequence-stratigraphic framework and incorporation of surface and subsurface data, hydrocarbon play element quality and distribution can be evaluated, which is critical for economic success.

Although there are numerous methodologies for employing genetic basin analysis, for this study, the Exxonian sequence stratigraphic model is utilized (Van Wagoner et al., 1990; Neal and Abreu, 2009; Abreu et al., 2010). In this model, the depositional sequence is the primary stratigraphic unit and is composed of three (3) systems tracts with characteristic parasequence stacking patterns and architecture (i.e., lowstand systems tract (LST) with progradation to aggradation parasequence stacking, transgressive systems tract (TST) with retrogradation parasequence stacking, and highstand systems tract (HST) with progradation to aggradation parasequence stacking). Moreover, three (3) effectively isochronous stratigraphic surfaces (i.e., sequence boundary (*sb*), transgressive surface (*ts*), and maximum flooding surface (*mfs*)) are identified and correlated where stacking of parasequences change, representing a significant shift in shoreline trajectory and depositional environments.

Parasequences are the fundamental building blocks of depositional sequences. A parasequence is defined as "a distinctive succession of relatively conformable beds and bedsets bounded by surface of flooding, abandonment, or reactivation and their correlative surfaces" (Van Wagoner et al., 1988; Abreu et al., 2010; Bohacs et al., 2014). Parasequences in shelfal settings can be subtly expressed, however, detailed observations indicate that they can be recognized through integrated sedimentologic criteria (i.e., lamina shape, continuity, bed thickness, sedimentary features, bioturbation index, and trace-fossil type and diversity) which is greatly aided by core control near surface exposures (Schieber and Lazar, 2004; Bohacs et al., 2005, 2014; Schieber and

Wilson, 2013; Lazar et al., 2015). A typical parasequence expression in mudstone-dominated strata includes coarsening-upwards packages that reflect shoreline progradation, commonly showing a secular decrease in organic-content, increased bioturbation intensity and trace-fossil diversity, as well as increase in bed thickness and products of higher energy deposition upsection (Macquaker et al., 1998; Bohacs et al., 2005, 2014). Parasequence boundaries (i.e., flooding surfaces) represent a nearly isochronous surface that subdivides more proximally deposited strata below from more distally deposited strata above, and are typically marked by increased abundance in pelagic input (i.e., conodonts, radiolarians, sphaeromorphic and acanthomorphic algal cysts), decreased bioturbation intensity and diversity, increased lamina and bed continuity, finer-grained textures, as well as an increase in authigenic/diagenetic cements and nodules (Bohacs et al., 2005; Lazar et al., 2015). It is critical to understand the expression and spacing of the development of parasequence boundaries to establish parasequence-set trends and system tract development.

System tract boundaries are identified through correlation of parasequences and termination styles of parasequence boundaries (onlap, downlap, toplap, or truncation). Through mapping vertical and lateral expression of parasequences, parasequence-set-scale observation provide the key ingredients for evaluation at the depositional sequence scale (i.e., LST, TST, HST). It is at the depositional sequence- and sequence-set-scale where observations and analysis can be validated at the scale of reflection seismic data (10's of meters). For these reasons, among others, it is necessary to integrate surface with subsurface data, including detailed descriptions of facies and facies associations along with parasequence expression and stacking patterns to facilitate building a comprehensive sequence stratigraphic framework.

Sub-surface mapping was conducted using IHS Petra® software with seismic and digital wireline log data provided by the Empire State Organized Geologic Information System (ESOGIS). Initially, geologic tops of key horizons were correlated throughout the basin, which later developed into defining high-resolution sequence stratigraphic packages based on stratal architecture, stratal geometry, stratal terminations, facies, and facies associations through integration of core and outcrop observations (Fig. 5). Total gamma ray and density logs are used to identify zones of organic-matter enrichment and gas potential, which can be identified as favorable areas for exploration and development. As a result of the extensive data collection of Devonian organic-rich shales as a result of the Eastern Gas Shales Project (EGSP), empirical relations between elevated total gamma ray response and both gas production and total gas content was established (Adams and Weaver, 1958; Harper and Abel, 1980; Schmoker, 1981). Therefore, mapping the net footage of elevated total gamma ray can be used to assess net "organic-rich pay" (ORP).

4. Results and interpretation

Detailed facies association characterization resulted in a facies framework for the Geneseo on the basis of critical physical, chemical, and biologic attributes (Wilson and Schieber, 2015). Through the documentation of texture, bedding, bedding thickness, composition, bioturbation index, and trace-fossil diversity, observed at hand sample scale and augmented through thin-section analysis, the resulting framework was vetted systematically within a genetic framework. Facies associations are delineated into the following categories:

FA1: Distal Organic-Matter-Rich Mudstones
FA2: Distal Organic-Matter-Rich Silty Mudstones and Argillaceous Siltstones
FA3: Medial Organic-Matter-Lean Silty Mudstones
FA4: Medial to Proximal Calcareous Silty and Sandy Mudstones
FA5: Medial to Proximal Argillaceous Siltstones and Sandstones

The facies associations summarized below record a depositional
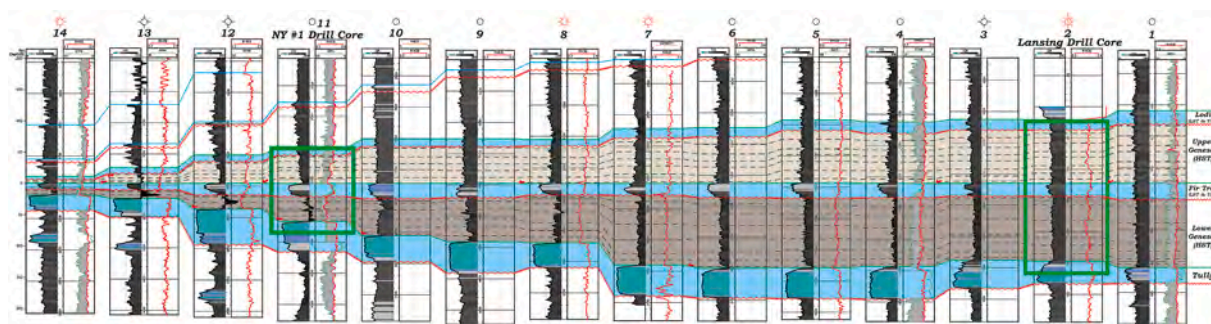
Fig. 5. Cross-section of Geneseo Formation (line from Fig. 4) showing a general thinning to the east. The Lower Geneseo Member downlaps/onlaps the Tully Formation/Hamilton Group (*mfs*), and shows aggradational-progradational stacking patterns (HST). In most places, the Lower Geneseo is truncated by a calcareous medium gray mudstone (commonly referred to as the Fir Tree Member). The Upper Geneseo downlaps/onlaps above this carbonate rich interval, and shows aggradational-progradational stacking patterns (HST), and is truncated by the overlying Lodi Member. Green boxes highlight two key cored wells.

system with systematic variations in depositional conditions, bottom water energy and oxygen levels. Variations of physical, chemical, and biologic characteristics indicate changes from extremely distal zones dominated by biogenic primary production to areas relatively proximal to siliciclastic shorelines dominated by clastic dilution. The majority of the strata accumulated along a profile through a storm-wave-dominated shelf, especially in the interval of the Lower Geneseo Member. In contrast, the upper part of the Upper Geneseo Member and Sherburne equivalent appears to have accumulated in a river-flood-dominated shelf environment (Bridge and Willis, 1991, 1994; Wilson and Schieber, 2017a). The following section details these facies associations in terms of recognition criteria.

4.1. Distal Organic-Matter-Rich Mudstones (FA-1)

Observations: Lamina geometries observed consist of planar, continuous and discontinuous lamina and lamina-sets with subtle inclined terminations (Fig. 6). Erosional scours are common, but are subtly expressed due to a lack of textural and compositional variation (Figs. 6A and 7). Grain sizes range from clay to fine silt (2–20 μm), with silt particles dominated by sub-rounded to rounded quartz (50%), calcite (35%), mica (10%), and feldspars (5%). Bed thickness ranges from 1 to 15 mm (dominantly <10 mm). Trends of bed thickness within bedsets are predominantly aggradational (75%), fining- and thinning-upwards bedsets comprise 15%, and coarsening- and thickening-upward bedsets comprise 10%.

Bioturbation indices range from 0 to 3 (dominant BI = 1) with bioturbation occurring primarily in the horizontal plane (meioturbation). Large macroburrows are sparse and this facies displays low trace-fossil diversity, but does include agrichnia (Wilson et al., 2021), *Chondrites*, *Helminthopsis*, *Planolites*, and *Phycosiphon*. Benthic macrofauna are uncommon, however, abundant agglutinated benthic foraminifera and benthic fecal pellets are observed (Fig. 8).

Elevated TOC content is observed and ranges from 1.8 to 8.1 wt% (ave. 3.89 wt) with high preservation and low degradation of OM. Enrichment of redox-sensitive trace elements are observed (Fig. 9), along with decreased detrital-proxy elements and more negative carbon isotope concentrations (ave. $\delta_{13}C_{org}$ −29.7‰). Si/Zr ratios are elevated in FA-1, reaching maximum values of 3.1 (ave Si/Zr = 2.3).

OM porosity dominates this facies, developed as nanopores that occur in kerogen particles and organo-minerallic aggregates (10–500 nm wide; Fig. 10). Phyllosilicate framework (PF) porosity is less common, however, where present shows the largest pores of this facies (up to 1500 nm wide). PF pores consist of triangular voids that are defined by a clay mineral framework. These pores are best developed in pressure shadows between and adjacent to larger and compaction-resistant grains (i.e., pyrite, quartz, calcite) and in compaction protected spaces between such grains (Fig. 11). Diagenetic mineral growth (quartz, dolomite,
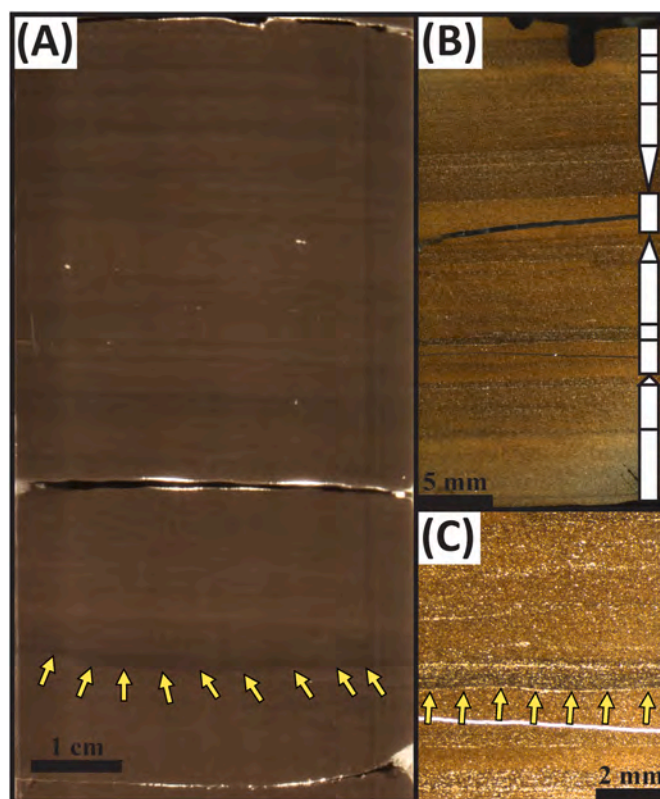
Fig. 6. (A) Image of polished hand sample (contrast enhanced) of the banded grayish-black mudstone facies, showing a subtle erosional scour infilled with darker muds (arrows). (B) Photomicrograph showing predominant horizontal banding with alternating light and dark layers with subtle erosional scours and continuous to discontinuous silt laminae caused by bottom-current sorting and transport. The alternating light and dark layers are interpreted to reflect fluctuating intensity of bioturbation produced by very shallow burrowing meiofauna and surface-grazing organisms such as polychaetes and nematodes. (C) Overview image of thin section with continuous to discontinuous, planar-parallel silt lamina/laminasets with scoured bases (arrows).

pyrite) also enhances PF pores by "clamping" clay flakes in place prior to compaction (Schieber, 2013; Wilson and Schieber, 2016) or by acting as a proppant that prevents collapse of triangular openings (Fig. 11).

Interpretations: FA-1 accumulated in a very distal shelf to basinal setting under relatively low-energy regime with high primary productivity and low clastic dilution under persistently dysoxic to intermittently anoxic bottom water conditions. These conditions were recorded in aggradationally stacked beds and bedsets of thinly bedded fine-
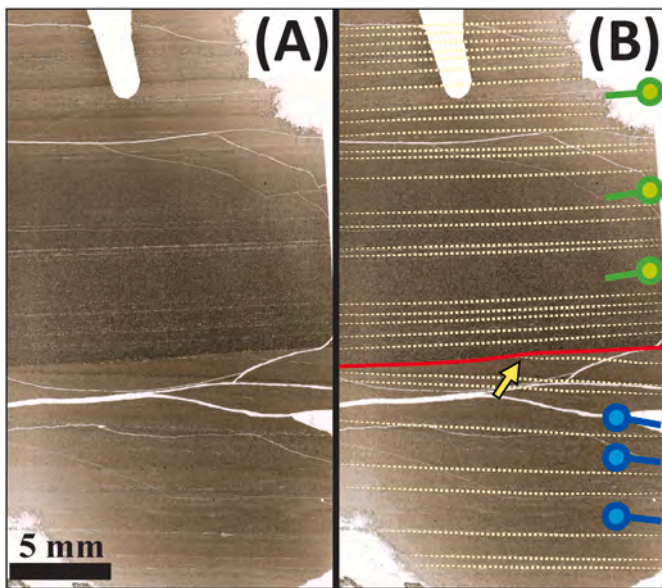
Fig. 7. (A) Photomicrograph of FA-1, note the alternating light and dark "bands" that are sub-divided by silt laminae and erosional scours. (B) Same photomicrograph used for (A) with overlay of lamina geometry (dashed yellow lines) and a subtle angular truncation (red line) subdividing beds above and below with opposing apparent bed dips (blue and green symbols). These features are commonly observed in thin-sections of the Geneseo organic-rich succession, however, they are not apparent in outcrop and core due to a lack in textural and compositional attributes. (For interpretation of the references to colour in this figure legend, the reader is referred to the Web version of this article.)

grained, pyrite-bearing, organic-matter-rich terrigenous and calcareous mud. Terrigenous mud is sourced from the east as offshore-directed bottom currents transported siliciclastics westward (Ettensohn, 1985). There appears to be (very) minor input of calcareous mud, potentially sourced from west in distal areas of the Geneseo as structural highs may have provided localized carbonate factories, thus, more mixed

carbonate-clastic mudstones are observed with increasing proximity to local carbonate factories to the west. Anoxic conditions did not prevail as evidenced by the abundance of agglutinated benthic foraminifera (Schieber, 2009) and benthic fecal pellets which consist of a mixture of silt and clays that were ingested by sediment-feeding organisms (Fig. 8), as well as meioturbation (Schieber and Wilson, 2021). Previous studies have speculated that fine-lamination in organic-matter-rich mudstones in the Geneseo, as well as other mudstone successions, is evidence that anoxia prevailed and prevented any bioturbation from benthos (Etten-sohn, 1987; Baird and Brett, 1991; Formolo and Lyons, 2007; Boyer et al., 2014). However, studies of modern muddy environments, as well as experimental studies provide alternative interpretations for fine-lamination in mudstones unrelated to bottom-water oxygenation levels. In the modern Gulf of Mexico, it has been documented that linking anoxia to bioturbation intensity in offshore muds can be a challenge as there is a preference by benthic organisms to settings with dissolved oxygen contents >80% (Dashtgard et al., 2015). Therefore, nonbioturbated mudstones may not be direct evidence for anoxia, rather, may record slightly lower oxygenation levels (60%–75% DO; Dashtgard et al., 2015; Dashtgard and MacEachern, 2016). Depositional processes were dominated by bottom-traction transport via persistent offshore-directed currents as evidenced by the presence of current ripple lamination and silt-lamina terminations. Moreover, SEM analysis reveals densely packed fabric interpreted to result from compaction of
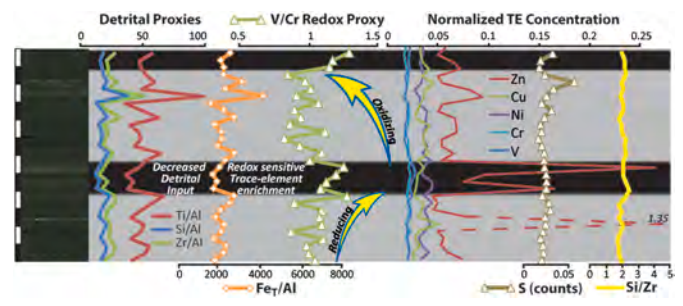
Fig. 9. XRF profile for FA-1 with detrital and redox proxies illustrated (white and black scale bars represent 1 cm each).
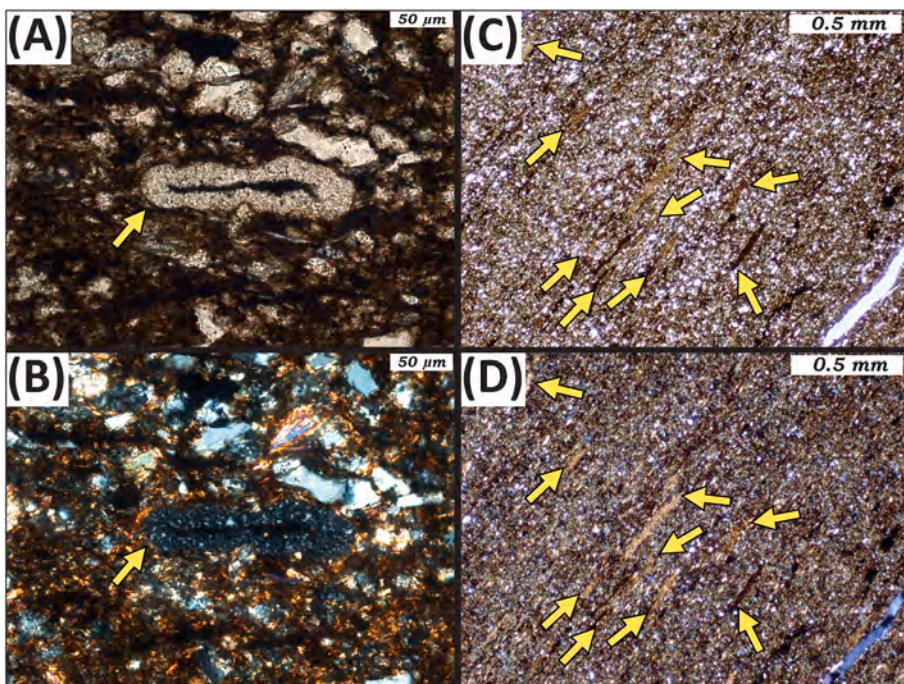
Fig. 8. (A) Photomicrograph showing agglutinated benthic foraminifera (yellow arrow) with partial internal fill that prevented complete collapse (plane-polarized light). Foraminifera are eukaryotic organisms, and as such require some oxygen to persist (Schieber, 2009). They are very common in the Geneseo Formation, and are distinguished by the lenticular assemblage of detrital quartz grains typically smaller than 10 mm. (B) The same image of (A) in cross-polarized light. The foraminifera consists of tiny gray birefringent quartz grains with internal fill preserved. (C) and (D) Scattered benthic fecal pellets in the mudstone matrix (plane and cross-polarized light, rotated 45°). The pellets (yellow arrows) are flattened by compaction, and consist of a mixture of silt and clays that were ingested by sediment-feeding organisms. The presence of benthic life is confirmed by the common presence of benthic fecal pellets and benthic agglutinated foraminifera in these strata. (For interpretation of the references to colour in this figure legend, the reader is referred to the Web version of this article.)
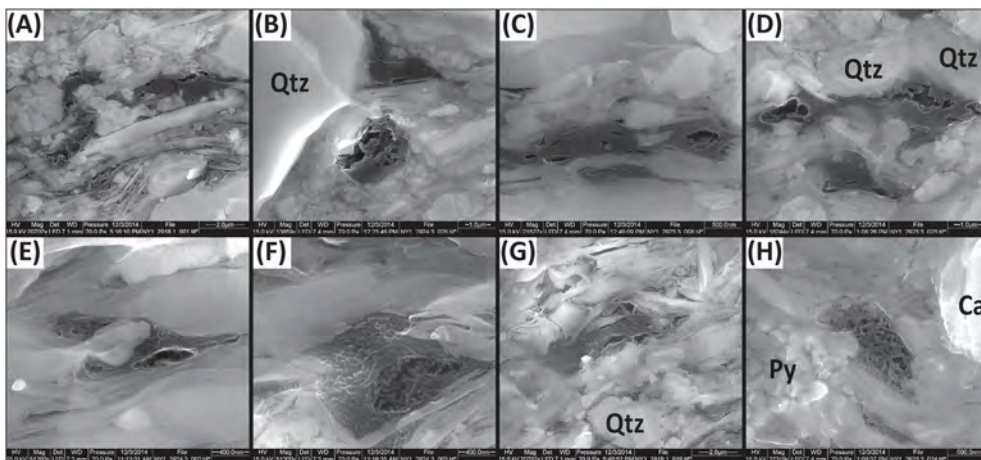
Fig. 10. Secondary electron images showing examples of OM porosity in FA-1 resulting from thermal cracking of labile organics and subsequent migration of hydrocarbons to infill nearby open porosity (arrows). Continued pressure and temperature allows further development of kerogen and bitumen micropores. Kerogen particles fill primary PF framework porosity, thus it is essential for compaction-resistant grains such as quartz (Qtz), calcite (Ca), or pyrite (Py) to be present in shale matrix for pressure envelopes to preserve open phyllosilicate porosity.
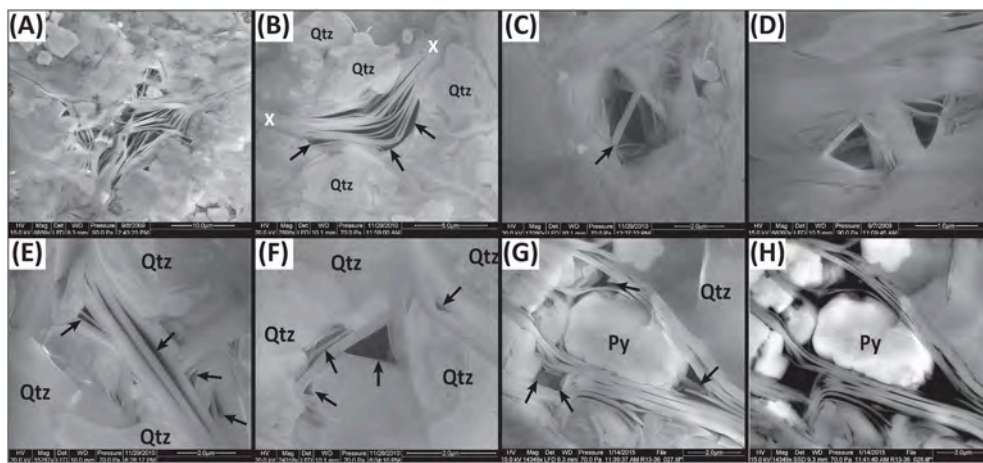
Fig. 11. Secondary electron images showing examples of PF framework porosity where dispersed quartz (Qtz) silt grains create pressure shadows that allow for only partial collapse of original phyllosilicate fabric (arrows). PF pores are triangular openings that reflect pre-compaction grain orientations.

flocculated clays with abundant edge-face organization of clay-platelets, similar to fabrics produced through unidirectional flows of muddy suspensions in flume experiments (Schieber, 2009; Schieber, 2011).

Si/Zr ratios were used to identify relative contributions of detrital vs biogenic/authigenic quartz, with elevated values indicating more biogenic/authigenic sources of quartz due to lack of heavy mineral fractionation associated with detrital clastic grains (Wilson et al., 2020). Therefore, elevated values indicate elevated biosiliceous materials and/or authigenic quartz cements. Quartz overgrowths are observed commonly in FA-1 (Fig. 12). This relation is further supported by the
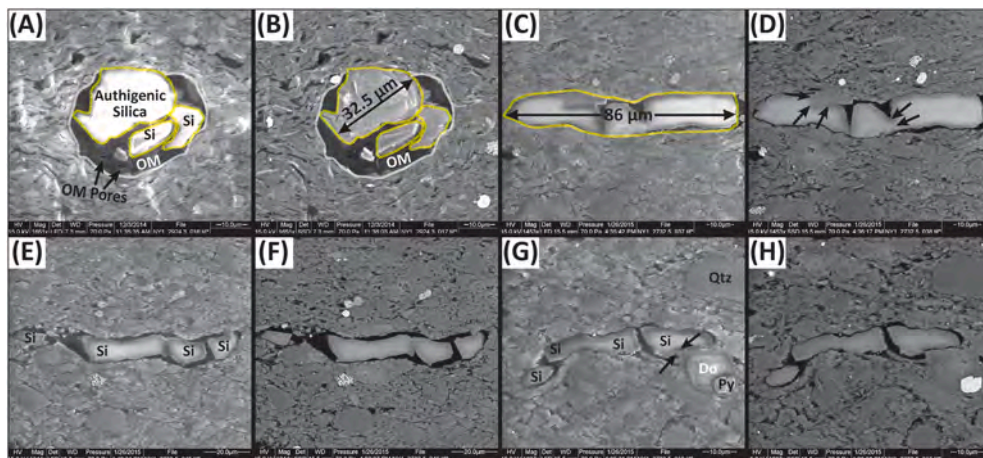
Fig. 12. A, C, E, G (Secondary Electron Images), and B, D, F, H (Backscatter Electron Images) showing examples of authigenic quartz cements, note the relationship with algal cysts which stiffen the rock to form high modulus fabric. Authigenic quartz may be the source of quartz silt/sand in distal, sediment starved environments. Authigenic quartz is critical for development of high modulus framework for brittle failure upon stimulation for unconventional reservoirs.

abundance of microalgae and pelagic microorganisms observed in thin-section and SEM, indicating high primary production and very slow sediment accumulation (Fig. 13). Concentration of microalgae associated with isotopically light (negative) organic carbon indicates the development of highly productive surface waters. Elevated surface-water productivity, decreased clastic dilution, and persistent dysoxic to sub-oxic conditions resulted in elevated TOC for this facies association. Early diagenetic calcite and pyrite in the form of nodules and concretions indicates slow and intermittent sediment accumulation and anoxic conditions in the sediment column (with the redox gradient likely occurring at very shallow depths just beneath the sediment–water interface). Preservation of uncollapsed algal cysts with fine morphologic details of original structure through early diagenetic reactions implies that mineralization operated rapidly and at a rate sufficient to outpace at least some post-mortem decomposition and decay (Fig. 13). Furthermore, the presence of uncompacted burrows in cemented horizons indicate rapid cementation prior to compaction and dewatering.

4.2. Distal Organic-Matter-Rich Silty Mudstones and Argillaceous Siltstones (FA-2)

Observations: Organic-matter-rich silty mudstones and muddy siltstones of this succession show wavy and planar, continuous and discontinuous lamina and lamina-sets with subtle inclined terminations (Fig. 14). Grain sizes range from clay to silt (2–40 μm), with silt particles dominated by sub-rounded quartz (70%), calcite (10%), feldspars (10%), and mica (10%). Dominant sedimentary features include current, wave, and combined-flow ripples with irregular basal scours. Lamina-set normal grading with evidence of wave modification and reworking is commonly observed. Bed thickness ranges from 10 to 35 mm (dominantly 25 mm). Trends of bed thickness within bedsets are predominantly aggradational (50%), fining- and thinning-upwards bedsets comprise 40%, and coarsening- and thickening-upward bedsets comprise 10%.

Bioturbation indices range from 0 to 3 (dominant BI = 1) with bioturbation occurring primarily in the horizontal plane. Large macroburrows are commonly observed as this facies displays moderate trace-fossil diversity, consisting of navichnia traces, *Chondrites*, *Planolites*, and *Phycosiphon*. Benthic macrofauna are uncommon, but agglutinated benthic foraminifera and benthic fecal pellets are abundant.

TOC contents range from 1.3 to 4.7 wt% (ave. 2.4 wt%) with high preservation and low degradation of organic matter. Enrichment of redox sensitive trace elements are observed, along with elevated detrital elements and more negative carbon isotope concentrations (ave. $\delta_{13}C_{org}$

−28.9‰). Si/Zr ratios reach maximum values of 2.65 (ave Si/Zr = 1.9). Authigenic silica cements are common throughout this facies as silica spheres in algal cysts as well as quartz overgrowths, there is, however, more terrigenous quartz silt compared to FA-1. Natural fractures are abundantly observed with fractures commonly filled with calcite or bitumen. Pore types include both interparticle and OM porosity, particularly developed inside organo-minerallic aggregates. FA-2 is composed of a mixed pore system with elevated organic content that allows the development of extensive OM porosity which appears intimately related with the interparticle porosity (IP).

Interpretations: This facies association records deposition in the distal shelf setting in a relatively higher energy regime compared to FA-1 with high primary productivity, persistently dysoxic to intermittently anoxic bottom-water conditions, and moderate clastic dilution. FA-2 records these conditions in aggradational stacking of beds and bedsets of with high vertical heterogeneity (thinly bedded). Depositional conditions were similar to those of FA-1: persistently dysoxic with episodic anoxia and bottom-traction-dominated transport, but with more common high-energy events (Fig. 15). Natural fractures are commonly observed siliceous facies, and interestingly many fractures are filled with bitumen, suggesting high expulsion efficiency of FA-2 (Fig. 15B).

The abundance of microalgae, pelagic microorganisms, and authigenic-quartz overgrowths, as well as isotopically light (negative) organic carbon indicate high primary production with more moderate siliciclastic accumulation rates than FA-1. Organic-matter enrichment of these distal outer-shelf strata was most likely a result of highly productive surface waters in combination with decreased clastic dilution and persistently dysoxic to sub-oxic conditions. Sediment accumulation appears to have been more consistent than FA-1 due to the decreased presence of large early diagenetic nodules and concretions. However, diagenetic cements and overgrowths are more equally distributed throughout the rock matrix, indicating a non-stationary redox boundary with slightly higher rates of sediment delivery.

4.3. Medial Organic-Matter-Lean Silty Mudstones (FA-3)

Observations: This facies association comprises planar to wavy, continuous and discontinuous lamina and lamina-sets with abundant sedimentary features. Grain sizes range from clay to silt (2–40 μm), with silt particles dominated by sub-rounded quartz (65%), feldspars (20%), and mica (15%). Dominant sedimentary features include current, wave, and combined-flow ripples with irregular basal scours. Normal and inverse grading are present, together with hummocky cross-lamination and terrestrial phytodetritus, internal scours, and soft-sediment
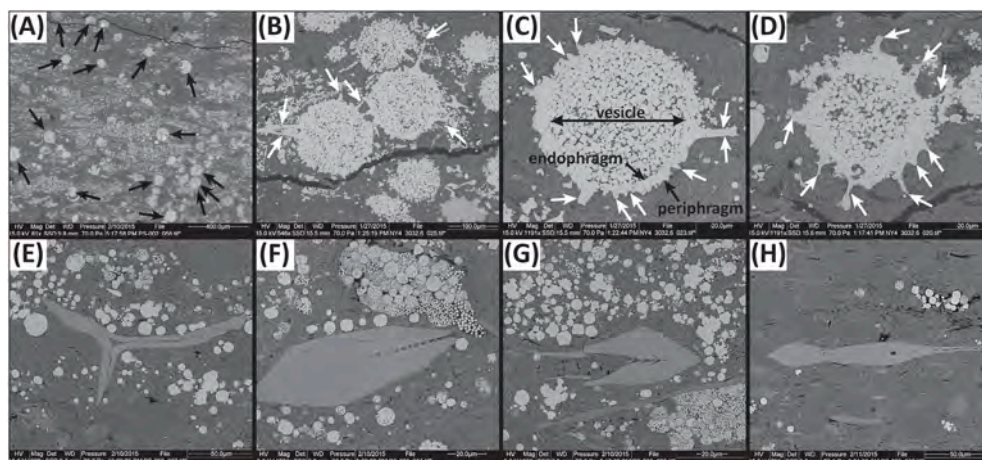
Fig. 13. Backscatter electron images illustrating pelagic inputs and evidence for sediment starvation, including (A–D) pyritized pelagic microfossils (i.e., styliolinids, radiolarians, sphaeromorphic and acanthomorphic algal cysts) and conodonts (E–H) with fine morphologic details of original structure (white arrows). Enrichment in pelagic microfossils and enrichment of pyrite framboids and polyframboids are key indices for sediment starvation at flooding surfaces.
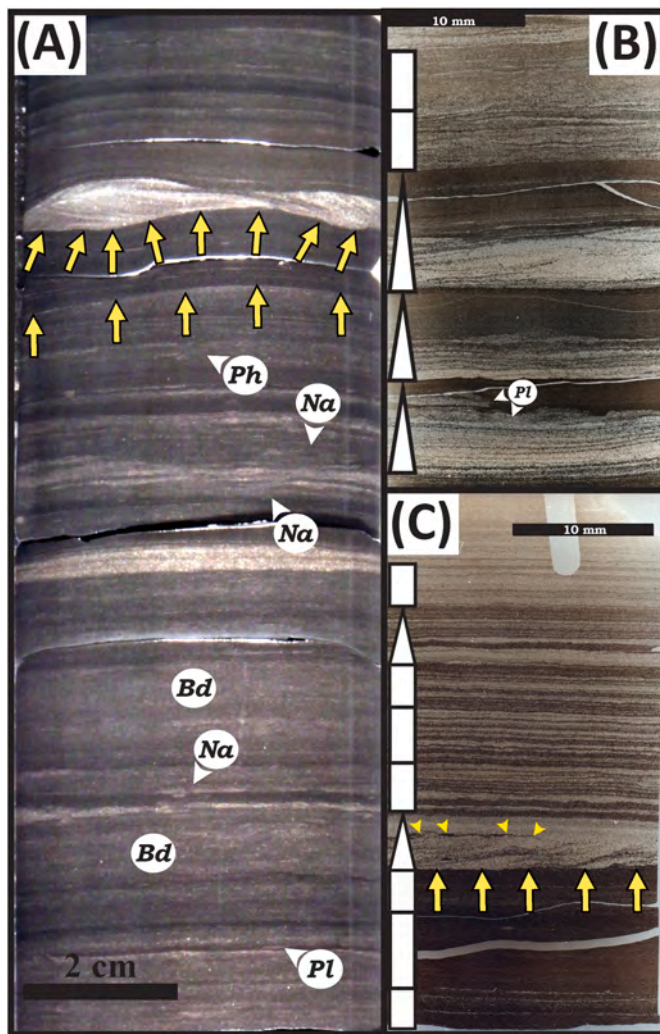
Fig. 14. A) Hand-sample image (contrast enhanced) of FA-2 showing erosional features (yellow arrows), current ripples, wave ripples with arcuate scalloped topography (white arrows), lamina-set grading, disrupted lamina, and bioturbation and biodeformational structures. The DGM facies contains biodeformation (Bd), navichnia traces (Na), and a suite of ichnogenera including *Planolites* (Pl), *Phycosiphon* (Ph). The increase in bioturbation intensity (BI 3–4) suggests that aerobic conditions prevailed, and that the redox boundary was located deeper below the sediment surface. B) Photomicrograph showing this facies with several graded beds. At the base are planar-laminated to low-angle cross-laminated silt-rich beds that fine upwards into sparsely to moderately bioturbated (BI 2–3) dark gray mudstone. These graded beds probably represent distal tempestites, where storm waves suspended and transported shelfal muds offshore. C) Photomicrograph showing this facies with current ripples, continuous planar silt laminae, and amalgamation. An interesting observation is the bundling of silt laminae upsection and an overall coarsening upwards trend which probably reflects a more proximal environment (coarser clastic influx) with extensive current reworking. (For interpretation of the references to colour in this figure legend, the reader is referred to the Web version of this article.)

deformation (Fig. 16). Bed thickness ranges from 10 to 75 mm (dominantly 10–30 mm). Beds and bedset stacking are predominantly coarsening- and thickening-upwards (75%), with lower frequency of aggradational (20%) as well as fining- and thinning-upwards (5%).

A wide range of bioturbation indices are observed (BI = 0–5), however, the most common BI is = 3 and about 75% of burrows are horizontally aligned, the remainder are inclined. A high diversity of trace-fossil ichnogenera are observed, consisting of navichnia traces, fugichnia (escape) traces, *Palaeophycus*, *Phycosiphon*, *Planolites*, *Thalassinoides*, and *Teichichnus*. Furthermore, an increased benthic fauna
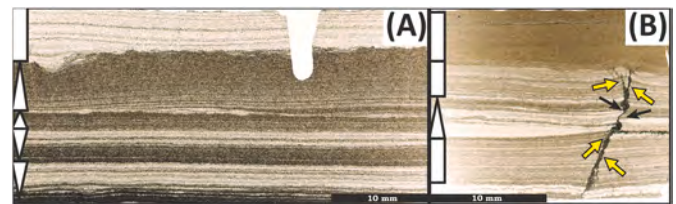
Fig. 15. A) Photomicrograph of FA-2 showing abundant planar-parallel and current-ripple lamination with basal scours and normal/inverse grading (white triangles on left). Note the thin-bedded nature to this facies showing alternations in siliceous mudstones and siltstones. B) Photomicrograph of FA-2 showing natural fracture (yellow arrows) with slight displacement (black arrows) with migrated hydrocarbons (bitumen). Note the termination of fracture at boundary with clay-rich shale illustrating a ductile fractard. Highly interbedded facies are associated with high expulsion efficiency and fracture complexity due to high compositional contrast at bed-boundaries. (For interpretation of the references to colour in this figure legend, the reader is referred to the Web version of this article.)

diversity is observed with frequent colonizations of disarticulated *Orbiculoidea lodiensis* and *Leiorhynchus* along bedding planes (Fig. 17).

TOC contents ranging from 0.3 to 1.8 wt% (ave. TOC = 0.8 wt%) with low preservation and moderate degradation of OM. These characteristics result in an intermediate/non-descript total-gamma-ray well-log signature. Enrichment of detrital-proxy elements are observed, along with decreased redox sensitive trace elements and less negative carbon isotope values (ave. $\delta_{13}C_{org}$ −28.1‰). Authigenic quartz proxy Si/Zr ratios are lower in FA-3, reaching maximum values of 2.15 (ave Si/Zr = 1.8). PF pores dominate FA-3, with OM pores contributing minimally to the total porosity observed.

Interpretations: FA-3 records deposition in a medial storm-wave-dominated shelf setting with moderate to low rates of primary production, persistent oxia, and higher clastic-flux rates than FA-2. Rapid deposition of thinly interlaminated siltstones and mudstones above storm-wave-base is evident due to the abundant erosional scours, lag development, and hummocky cross-lamination. Higher clastic influx rates and persistently oxic conditions resulted in overall low organic-contents in FA-3, due to oxidation and consumption of organics by benthos as evidenced by elevated bioturbation indices as well as increased diversity of benthic fauna and trace fossils. Beds and bedset stacking are predominantly coarsening- and thickening-upwards (75%), with lower frequency of aggradational (20%) as well as fining- and thinning-upwards (5%). Si/Zr ratios indicate more detrital quartz grains and less biogenic/authigenic silica than FA-1 and FA-2. Additionally, heavier (less negative) carbon isotope values suggest more terrestrial derived phytodetritus, as well as more oxidized organic matter due to destruction.

Depositional processes are interpreted to have been dominated by storm deposition and remobilization of shelf muds for offshore-directed transport as evidenced by the abundance of erosional features, amalgamation, and wave-modified current-ripples (combined flow). Current and wave-enhanced sediment-gravity flows may have contributed significant volumes of sediment to the medial shelf setting. In particular the current- and wave-aided hyperpycnal flows can spread fluvial discharge over 100's of kilometers (Wilson and Schieber, 2014).

Wide ranges in bioturbation index appear to have been a result varying sedimentation rate rather than redox conditions, as intervals with more intense bioturbation (BI = 3–5) are associated with higher clay content with overall lower siltstone interlaminations. This relation suggests more rapidly deposited discrete coarse-mudstone beds have higher preservation potential due to rapid burial than more slowly accumulating fine-mudstone beds which are exposed longer to biogenic disturbance. Variations in sediment flux was likely a result of relative sediment starvation between depositional events.
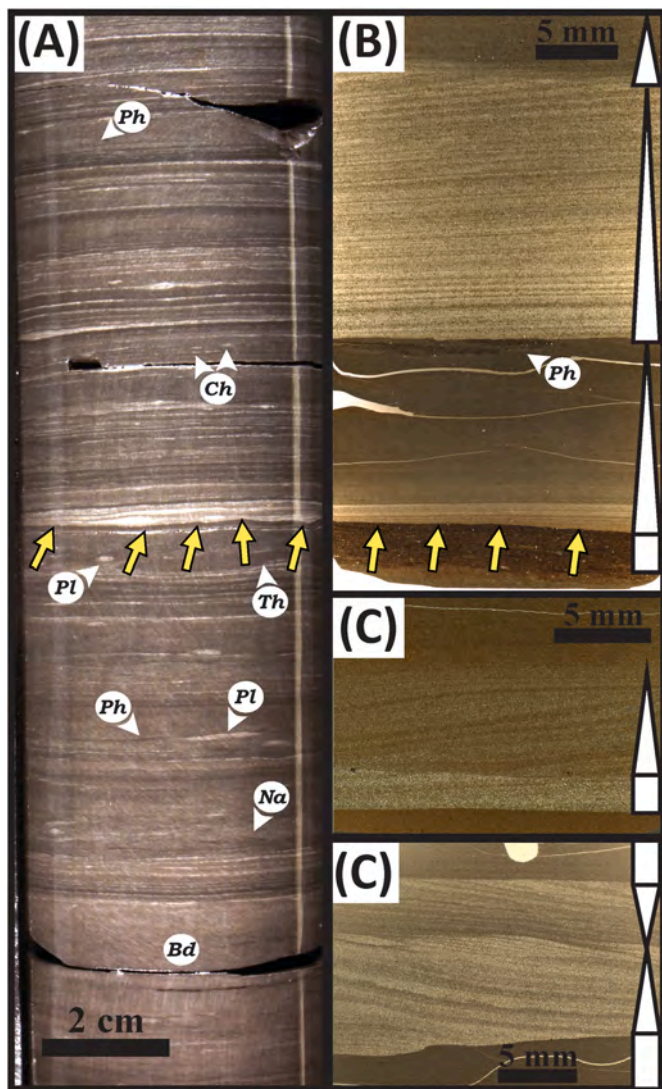
Fig. 16. A) Hand-sample image (contrast enhanced) of FA-3 showing erosional scours, current ripples with low-angle cross-lamination, normal and inverse lamina-set grading, and varying degrees of bioturbation. FA-3 contains bio-deformational (Bd) features and navichnia traces (Na), as well as a suite of ichnogenera including *Planolites* (Pl), *Thalassinoides* (Th). The increase in bio-turbation intensity (BI 5 4–5) and diversity indicates that aerobic conditions prevailed. B) Photomicrograph showing styliolinid-rich dark mudstone with truncation surface that is overlain by low-angle cross-laminated silt onlapping on that surface. Planar-laminated silts grade upwards into *Phycosiphon* (Ph) burrowed dark mudstone (post-event background sedimentation). An erosional contact is observed above, with onlapping laminated silts, that grade upwards into inclined laminated silts with an increase in clay content. C) Thin graded bed with internal scour and current-ripple cross-lamination. D) Silt-rich hyperpycnite with basal scour and combined-flow ripples, indicating wave-aided transport (concave-up lamina-set geometries).

4.4. Medial to Proximal Calcareous Silty and Sandy Mudstones (FA-4)

Observations: This facies association is composed of wavy to curved, continuous and discontinuous lamina and lamina-sets with abundant physical sedimentary structures (Fig. 18). Grain sizes range from clay to very fine sand (2–100 μm), with silt- and sand-sized particles dominated by sub-rounded quartz (45%), calcite (40%), feldspar (10%), and mica (5%). Components are of mostly extrabasinal detrital and reworked intrabasinal detrital origin; grains are predominantly composed of quartz and feldspar and clay minerals, along with a few muddy intraclasts. Dominant sedimentary structures include current,

wave, and combined-flow ripples with irregular basal scours. Normal and inverse grading are present, together with terrestrial phytodetritus, internal scours, and soft-sediment deformation. Bed thickness ranges from 20 to 90 mm (dominantly 40 mm). Beds and bedset stacking are predominantly fining- and thinning-upwards (65%) with coarsening- and thickening-upwards (25%), and some aggradational (10%).

A range of bioturbation indices are observed (BI = 3–5) and the most common BI is = 3. About 50% of burrows are horizontally aligned, 30% are inclined, and 20% are vertical traces. A high diversity of trace-fossil ichnogenera are observed, consisting of navichnia traces, fugichnia traces, *Palaeophycus*, *Phycosiphon*, *Planolites*, *Thalassinoides*, and *Teichichnus*. Additionally, disarticulated and fragmented small brachiopods (Ambocoelia and Devonochonetes) (Thompson and Newton, 1987), pelmatozoans, ostracodes, and auloporid tabulate corals are present in this facies.

TOC contents ranging from 0.35 to 4.9 wt% (ave. TOC = 2.1 wt%) with moderate to high preservation, degradation, and dilution of organic material in this clastic-dominated setting. Elemental data shows mixed sources of sediment, particularly, increased carbonate content is apparent (up to 65 wt% $CaCO_3^{2-}$). Gamma ray log signature is typically intermediate and non-descript. Moderate carbon isotope values are observed (ave. $\delta_{13}C_{org}$ −28‰), and do not show significant variability. Authigenic quartz proxy Si/Zr ratios are lower in FA-3, reaching maxima values of 1.18 (Ave Si/Zr = 0.72). The dominant pore system observed in FA-3 is carbonate dissolution (CD) porosity (Wilson and Schieber, 2016).

Interpretations: FA-4 records deposition in a mixed-energy (Lin and Bhattacharya, 2020) medial to proximal storm-wave dominated shelf setting with moderate to high rates of primary production, within a dysoxic to oxic setting and fluctuating sedimentation rates. This transitional setting resulted from multiple processes overprinting through the combined effects of variable sediment supply and sediment bypass from the proximal prodelta to the distal shelf setting during progradation. Similar to FA-3, depositional processes were dominated by storm deposition, remobilization of shelf muds, and offshore-directed transport. Rapid deposition of fine-grained mudstones and very fine sandstones above storm-wave base is suggested by the abundant erosional scours, lag development, and hummocky cross-lamination. This medial to proximal shelf environment had overall low organic-matter content, most probably due to the combination of moderate to low rates of primary production, poor preservation, and moderate to high dilution.

Additionally, heavier (less negative) carbon isotope values suggest more terrestrially derive phytodetritus than FA-1 or FA-2, as well as more oxidized organic matter due to destruction. Si/Zr ratios indicate elevated contribution of detrital quartz grains in comparison to FA-1 and FA-2. FA-4 is primarily observed in the Fir Tree member of the Geneseo Formation.

4.5. Medial to Proximal Argillaceous Siltstones and Sandstones (FA-5)

Observations: This facies association comprises parallel and nonparallel wavy to curved, discontinuous lamina and lamina-sets with abundant sedimentary features (Fig. 19). Grain sizes range from clay to very fine sand (2–100 μm), with silt- and sand-sized particles dominated by sub-rounded quartz (75%), feldspar (20%), and mica (5%). Components are of mostly extrabasinal detrital and reworked intrabasinal detrital origin; grains are predominantly composed of quartz and feldspar and of clay minerals, along with a few muddy intraclasts. Dominant sedimentary features include current, wave, and combined-flow ripples with irregular basal scours. Beds with normal and inverse laminaset grading are present, together with terrestrial phytodetritus, internal scours, soft-sediment deformation, and fluid-escape structures. Bed thickness ranges from 20 to 90 mm (dominantly 60 mm). Beds and bedset stacking are predominantly coarsening- and thickening-upwards (55%) with fining- and thinning upwards (30%), and aggradational
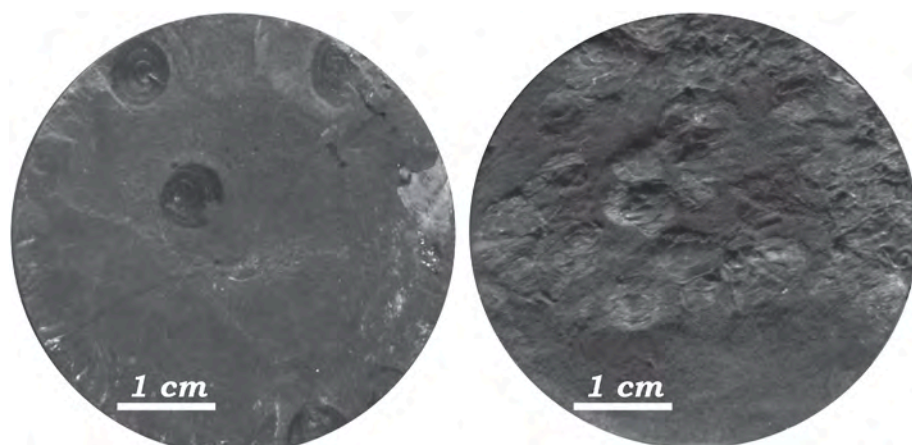
Fig. 17. View along core bedding planes with distinctive fauna. On the left are examples of flattened *Orbiculoides lodensis*, a linguliform brachiopod with small (typically <2 cm) circular valves. *Orbiculoides* groups are interpreted as epifaunal filter feeders and associated with dysoxic conditions. On the right are examples of *Leiorhynchus*, a rhynchonelliform brachiopod which is typically observed inflated to compressed with original shell material rarely preserved, instead they are preserved as flattened molds. Leiorhynchids are interpreted as epifaunal filter feeders, associated with dysoxic conditions.

(15%).

A range of bioturbation indices were observed (BI = 0–4), with the most commonly observed BI being = 0–1. About 60% of burrows are horizontally aligned, 30% are inclined, and 10% are vertical traces. A low diversity of trace-fossil ichnogenera are common, consisting of navichnia traces, fugichnia traces, *Palaeophycus*, and *Phycosiphon*.

TOC contents ranging from 0.12 to 0.47 wt% (ave. TOC = 0.29 wt%) with poor preservation and moderate to high degradation of OM. FA-5 shows dominantly detrital components as indicated by XRF data with elevated detrital-proxy ratios and low concentrations of redox-sensitive trace metals. Gamma ray log signature is commonly blocky with minimal to moderate radioactivity. Additionally, less negative carbon isotope values are observed in this facies association (ave. $\delta_{13}C_{org}$ −27.2‰). Authigenic quartz proxy Si/Zr ratios are lower in FA-5, reaching maximum values of 0.87 (ave Si/Zr = 0.67). Interparticle (IP) porosity dominate FA-5, with PF pores providing additional porosity in clay aggregates and rip-up mudstone clasts.

Interpretations: FA-5 records accumulation in a medial to proximal fluvially-influenced, storm-wave-dominated shelf setting under moderate to low rates of primary production, persistent oxic conditions, and elevated clastic flux. Rapid deposition of coarse grained mudstones and very fine sandstones above storm-wave-base is evident due to the abundant erosional scours, lag development, and hummocky cross-lamination. This facies association has a wider range of grain sizes than FA-4 due to proximity to fluvial discharge.

Overall organic-matter content is low due to low to moderate rates of production, high destruction, and moderate to high dilution. Bioturbation indices indicate oxic bottom- and pore-water docitions, however, bioturbation index variability and low trace-fossil diversity is observed abundantly. Additionally, heavier (less negative) carbon isotope values suggest more terrestrial derived phytodetritus, as well as more oxidized organic matter due to destruction. Spatial variations in sediment input, however, may have promoted localized enrichment of organic matter. Si/Zr ratios are the lowest of all the facies associations, indicating that detrital quartz grains are the dominant form of silica in FA-5.

In summary, FA-5 records rapid sedimentation rates and episodic input of freshwater from the Catskill deltaic source, both which act as ecologic stressors to benthos (Gingras et al., 2009; MacEachern and Pemberton, 1992; Bhattacharya and MacEachern, 2009).

5. Sequence-stratigraphic framework

Sequence stratigraphy is the subdivision of rocks into genetically related packages, bounded by key surfaces including unconformities and their correlative conformities (Van Wagoner et al., 1988). The building blocks of the depositional sequence are parasequences, which are relatively conformable beds and bedsets, bounded at the top and base by parasequence boundaries (i.e., flooding surfaces) (Van Wagoner et al., 1988). This section will first demonstrate parasequence expression, and then build into the depositional sequences that span the Lower and Upper Geneseo members.

5.1. Parasequence boundary expression

Observations: Genetically related beds and bedsets in the Geneseo Formation have been identified on the basis of physical, chemical, and biologic attributes (Fig. 20). Furthermore, proximal–distal relations are apparent within successive parasequence packages. The key stratigraphic surface to recognize at this scale is the parasequence boundary (i.e., flooding surfaces and lateral equivalents). Subdivision of genetically related beds and bedsets requires the demonstration that parasequence boundaries can be identified and correlated (Bohacs et al., 2005). Through the correlation of parasequence boundaries in the Geneseo Formation across the NAB, it was observed that their expression changes throughout the basin in relation to shoreline trajectory. For instance, in the proximal to medial realm, parasequence boundaries mark an abrupt change from underlying FA-5 to overlying FA-1. This drastic change is often reflected in the marked increase in total organic content and lamina continuity across this boundary, as well as a decrease in grain size (from fine sandstones to fine–medium mudstones), bed thickness, and bioturbation intensity. Furthermore, the intervals just above parasequence boundaries in this setting show an increase in pelagic flux with respect to detrital input. For instance, it is typical to observe enrichment in pelagic microfossils (i.e., radiolarians, styliolinids, acritarchs (i.e., sphaeromorphic/acanthomorphic algal cysts), prasinophytes (i.e., *Leiosphaeridia*, *Tasmanites*); Figs. 12 and 13).

Organic-walled microfossils are subject to post-mortem degradation that can modify or obliterate characteristics that are taxonomically significant, in an analogous manner to carbonate-walled macrofossils (Li et al., 2021). The microfossils observed at and above parasequence boundaries in this setting typically range from 80 to 150 μm in diameter, and are commonly preserved through varying degrees of pyritization and show signs of originally containing a flexible wall (Fig. 12). The diagenetic relations of microfossils provide significant information regarding sedimentation rates as well as rate of cementation in the substrate. Early diagenetic cements are encountered all throughout the Geneseo Formation. It is, however, often a topic of debate how early cementation commenced and the relative implications for position of the redox boundary. Bioturbation, agglutinated benthic foraminifera, and benthic fecal pellets all indicate the presence of dissolved oxygen at the seafloor, even if in small amounts (i.e., suboxic). However, when uncollapsed pyritized algal cysts are observed with fine morphologic detail indicating that mineralization of early diagenetic cements
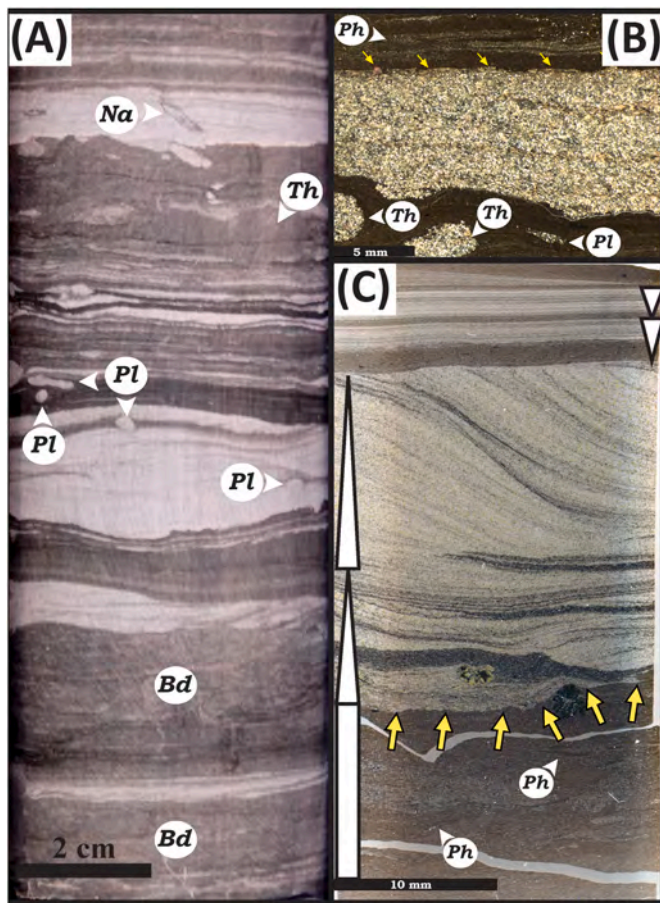
Fig. 18. A) Hand-sample image (contrast enhanced) of FA-4 showing increased erosional features, thick current ripples and wave ripples with arcuate scalloped topography, laminaset grading, disrupted lamina, and bioturbation and bio-deformational structures. FA-4 facies contains biodeformational (Bd) features and navichnia traces (Na), as well as a suite of ichnogenera including *Planolites* (Pl), and *Thalassinoides* (Th). The increase in bioturbation intensity (BI 4–5) suggests that aerobic conditions prevailed, and that the redox boundary was located deeper below the sediment surface. B) Photomicrograph (cross-polarized light) showing deep erosional scour, silt-filled *Planolites* (Pl) and *Thalassinoides* (Th) burrows, and reworked siltstone bed containing skeletal debris (disarticulated styliolinids and brachiopods). Note that the surface of siltstone bed is marked by styliolinids and pelmatozoan debris (yellow arrows). C) Photomicrograph showing FA-4, with the lower portion of the sample containing bioturbated styliolinid-rich mudstone, and an erosional contact with the overlying current-rippled interval that shows low-angle to high-angle cross lamination. Foresets of ripples contain abundant styliolinids and skeletal debris. The current ripple has an erosional cap and is overlain by planar laminated silts, suggesting that flow velocities waned after an initial erosive energy event. (For interpretation of the references to colour in this figure legend, the reader is referred to the Web version of this article.)

operated rapidly and at a rate sufficient to outpace at least some post-mortem decomposition and decay (Fig. 13).

The expression of parasequence boundaries in proximal to medial areas is rather obvious at the outcrop scale due to differential weathering of organic-matter-rich mudstones vs coarse-grained clastics (Fig. 20). The expression of parasequence boundaries in distal areas, by contrast, is less obvious in outcrop, making parasequences far less recognizable. Recognition of parasequence boundaries in distal settings requires much more detailed analysis of biologic attributes and diagenetic overprint to identify shoreline trajectory during parasequence formation. Parasequence boundaries in distal settings separate underlying moderately to strongly (BI = 3–4) bioturbated dark gray mudstones (ave. TOC = 1.7 wt%) from overlying nonbioturbated to weakly
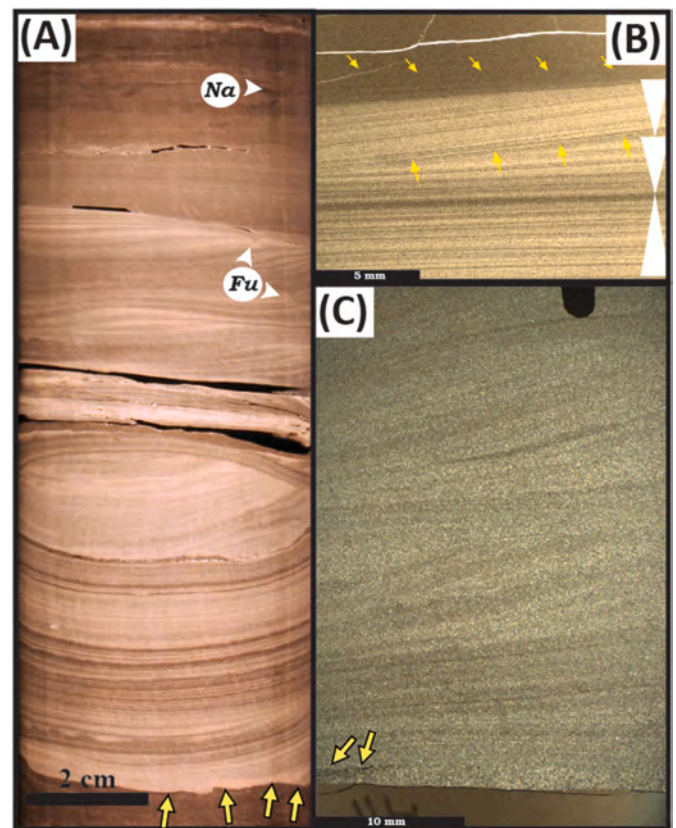
Fig. 19. A) Hand-sample image (contrast enhanced) of FA-5, showing erosional scours, current, wave, and combined-flow ripples, soft-sediment deformation (yellow arrows), normal and inverse lamina-set grading, and varying intensities of bioturbation. A variety of trace fossils are present, including fugichnia traces (Fu), navichnia traces (Na), *Planolites* (Pl), and *Phycosiphon* (Ph). B) Photomicrograph showing a wave ripple with escape traces (Fu), with an irregular basal scour into sandy mudstone with *Palaeophycus* (Pa) burrows. C) Another wave ripple with hummocky cross-lamination and scour overlying silty mudstones with fugichnia traces (Fu). Note the steepening-upward laminae in the upper two beds of this deposit, indicating modification or influence by unidirectional currents. (For interpretation of the references to colour in this figure legend, the reader is referred to the Web version of this article.)

bioturbated (BI = 0–1) grayish black mudstones (ave. TOC = 3.8 wt%). Moreover, early diagenetic cements and nodules are common at or just beneath flooding surfaces. Texturally speaking, there is not a significant shift in grain size across the boundary. Furthermore, carbon isotopes do not show significant variation due to the dominant marine (algal) contribution in the distal realm (Wilson and Schieber, 2017b). However, the upper beds of parasequences tend to have isotopically less negative organic matter than the basal beds of the same parasequence. This trend is interpreted to reflect slightly more oxidized organic material due to degradation and consumption by benthic organisms.

Interpretation: Enrichment of pelagic material appears to be a consequence of expansion of the photic zone as the shoreline retreats, resulting in a larger area for primary production. Additionally, decreased clastic input facilitates the enrichment of pelagic materials at the seafloor.

5.2. Parasequence expression

After recognition criteria have been set for identifying and correlating parasequence boundaries, genetically related beds and bedsets can be differentiated to develop a sequence stratigraphic framework and understand 3-D character and facies associations within a stratigraphic hierarchy. Throughout the discussion of Geneseo facies associations,
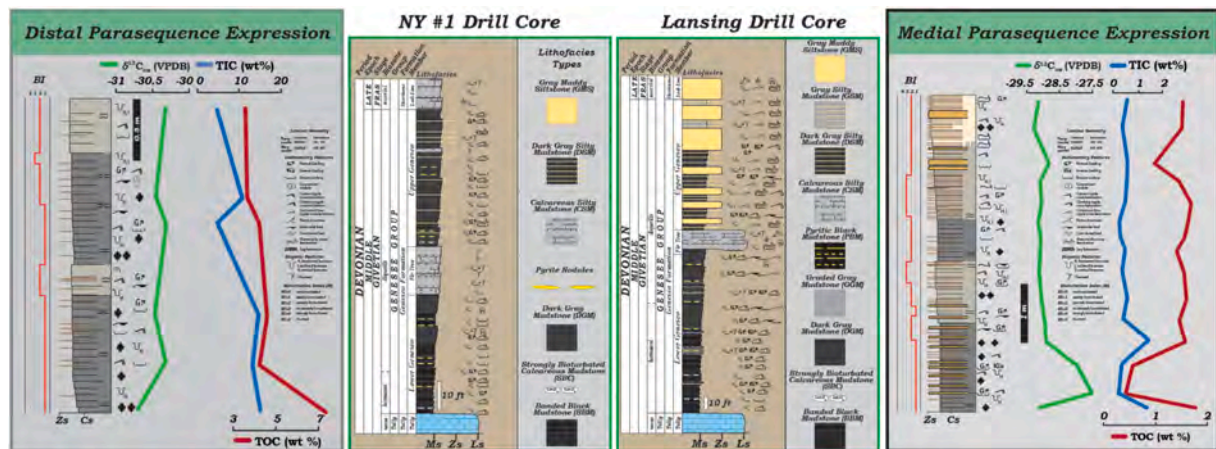
Fig. 20. Detailed descriptions of cored wells from Fig. 5 cross-section. Parasequences have been identified and correlated across the basin to assess facies distribution and stratal termination style. Generalized lithostratigraphy and sedimentary features observed for two (2) drill cores, the Lansing core representing more proximal setting, and the NY#1 core representing more distal setting. Parasequence expression includes physical features, bioturbation index (BI), carbonate percent (TIC), total organic-carbon content (TOC), bioturbation index (BI), and carbon isotopic composition of organic matter ($\delta^{13}C_{OM}$).

observations of bed thickness were addressed to make a connection with parasequence stacking.

Proximal to medial areas: Parasequences in the medial to proximal realm are expressed as coarsening-upwards beds and bedsets which demonstrate increased wave- and current-formed sedimentary features upsection (Fig. 20). This systematic trend is expressed through basal portions of parasequences that consist primarily of thinly bedded (banded) FA-1 and FA-2 with enrichment of marine dominated (algal) organic material (ave. $\delta^{13}C_{org}$ −29.7‰), elevated redox sensitive trace elements, early diagenetic cements and nodules, low bioturbation indices, as well as increased lamina continuity. Upsection, more thickly bedded FA-3 and FA-4 develop and dominate the parasequence expression proportionally with decreasing organic-content dominated by more terrestrial and oxidized marine organics (ave. $\delta^{13}C_{org}$ −27.2‰), increased terrigenous/coarser-grained material, and increased bioturbation indices are observed to an extent. Wherein fluvially-influenced FA-5 dominates, lower bioturbation indices are encountered with low trace fossil diversity, interpreted to be a result of ecologic stressors associated with high sedimentation rates and salinity changes.

Distal areas: In the distal setting, parasequences tend to be thinner (>50% decrease in thickness) and demonstrate more subtle vertical variations in mudstone facies, as FA-1 gradationally change to FA-2. Additionally, organic-matter contents in the distal setting are overall higher (ave. TOC = 3.8 wt%) in comparison to the medial and proximal setting (ave. TOC = 1.4 wt%) which is likely a function of increased levels of primary productivity as well as decreased clastic dilution. Basal portions of parasequences consist of thinly bedded (banded) FA-1 with enrichment of marine dominated (algal) organic material (ave. $\delta^{13}C_{org}$ −29.7‰), elevated redox sensitive trace elements, early diagenetic cements and nodules, low bioturbation indices, as well is increased lamina continuity. Upsection, a gradation transition to FA-2 is observed with increased bioturbation indices. The lack of textural contrast in distal parasequences impedes recognition, however, careful observation of bioturbation styles and intensity is the key discriminator.

These genetically related strata occur systematically within a broad depositional sequence, and aid in developing a high-resolution sequence-stratigraphic framework. Distinct facies associations occur vertically and laterally with characteristic stacking patterns that are associated with shoreline trajectory, sediment input, and accommodation. The Geneseo Formation contains meter-scale parasequences that progressively thin basinward and show stratal termination styles indicating shoreline progradation (i.e., downlap and onlap), shoreline retrogradation (i.e., onlap), and erosion association with sequence boundaries (i.e., toplap and truncation). As parasequences stack into

depositional sequences, organic-carbon enrichment occurs at the convergence of parasequences at the maximum flooding surface (*mfs*).

6. Depositional-sequence expression

High-resolution stratigraphy has allowed differentiation of genetically related strata, composed of distinct facies association with characteristic physical, biological, and chemical attributes. Correlation of this succession was conducted at the parasequence scale, and includes detailed descriptions of multiple drill cores and surface exposures, as well as subsurface mapping. The Geneseo Formation comprises portions of two depositional sequences. The Lower Geneseo Member overlies the Tully Formation, and where the latter is absent, its basal contact is commonly marked by a pyritic-phosphatic lag (the Leicester Pyrite Bed; *mfs*). This surface marks a significant flooding event that can be mapped basin-wide, resulting in basinal conditions that favor organic-matter production and enrichment of redox sensitive trace elements in the sediment column (Fig. 21).

Above this *mfs*, the Lower Geneseo Member shows aggradational to progradational parasequence stacking patterns that are indicative of a highstand systems tract (HST; Fig. 22) (Van Wagoner et al., 1988). Mapped parasequence boundaries show downlap/onlap terminations with the underlying *mfs* with enrichment of TOC, pelagic microfossils (i.e., styliolinids, radiolarians, sphaeromorphic and acanthomorphic algal cysts), as well as abundant early diagenetic cements (i.e., calcite, dolomite, pyrite, silica). Furthermore, the presence of inconspicuous discontinuous, bedding parallel pyritic streaks in basal bedsets of the Geneseo just overlying the *mfs*, interpreted as agrichnia traces (Wilson et al., 2021), indicates extremely slow sediment accumulation (condensed) and extremely oxygen stressed environments (suboxic). Isopach maps show westward thinning and pinchout of the HST to the west (cratonward). This pattern has been interpreted previously to represent downlapping of the Lower Geneseo onto a deep basin floor (100's of meters water depth). Conversely, this study presents an alternative model for correlating the Geneseo with a datum placed in the overlying strata which better portrays the impact of basement structures and geometries (correlation technique also employed in Smith et al., 2019). Herein, we propose that the Lower Geneseo lapped onto a series of positive structural elements westward in shallower water (10's of meters) than previously presumed. Moreover, thickness variation is observed throughout the basin along basement lineaments, suggesting a structural control on accommodation during deposition (Fig. 23). For instance, in Steuben and Chemung counties, drastic thickening towards south-central New York is observed in an area which corresponds to a
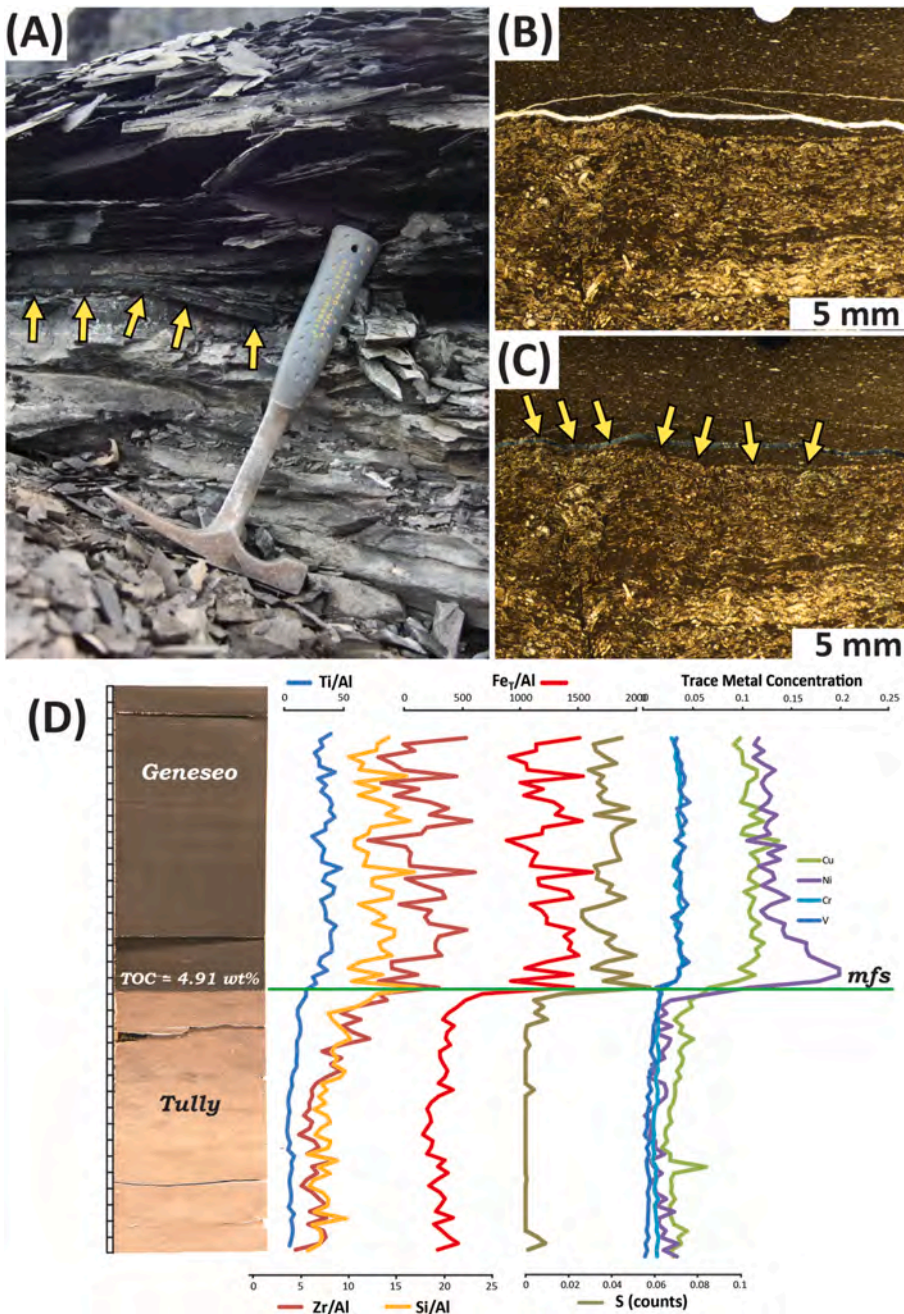
Fig. 21. A) Outcrop expression of the basal Geneseo *mfs* (yellow arrows) with a deep scour infilled with organic-rich muds. B) and C) Photomicrographs of the contact, note the drastic change in facies from styliolinid-rich packstone to organic-rich mudstones. D) Core example of this contact with detrital and redox proxies, note the enrichment of Cu, Ni, and V above the *mfs* with TOC enrichment. (For interpretation of the references to colour in this figure legend, the reader is referred to the Web version of this article.)

structural depression (Fig. 23). Therefore, correlation of parasequences show downlapping-onlapping to the west and terminate against basement structures, indicating these faults acted as sediment barriers/baffles. This structural control on accommodation is validated by field observations of the Lower Geneseo Member lapping onto an angular unconformity with the underlying Moscow Formation (bed orientation N14°E/4°SE). For example, at Cayuga Creek the underlying Moscow Formation shows tilted beds which are truncated and Geneseo laps onto this surface, suggesting structural deformation of previously deposited Moscow Formation (Fig. 24).

The Fir Tree Member unconformably overlies the Lower Geneseo Member and displays prograditional-aggradational-retrogradational parasequence stacking patterns (LST and TST) and consists of intervals enriched in FA-3 in the lower portion of the interval (LST), interfingering and grading vertically into predominantly FA-4 rich in disarticulated and fragmented auloporid tabulate corals, ostracodes, and

small brachiopods (TST), suggesting decreasing siliciclastic input. The unconformable contact between the Lower Geneseo Member and Fir Tree Member is interpreted as a sequence boundary (*sb*) with toplap terminations just beneath the surface and downlap/onlap terminations just above this surface (Fig. 25). Thickness variations in the Fir Tree Member (LST and TST) show a similar albeit muted trend as the underlying HST across the basin (Fig. 23). A general thinning to the west is observed and a thick in south-central New York associated with the convergence of two major basement faults that form a structural depression. Above the Fir Tree Member, the Upper Geneseo displays aggradational to progradational parasequence stacking patterns (HST) and consists of dark gray silty mudstones and muddy siltstones with abundant wave/current ripples, graded beds, and evidence for extensive reworking and erosion. Upper Geneseo parasequences show characteristic thinning westward, as well as downlapping-onlapping terminations with the underlying Fir Tree Member. Thickness variations in the Upper
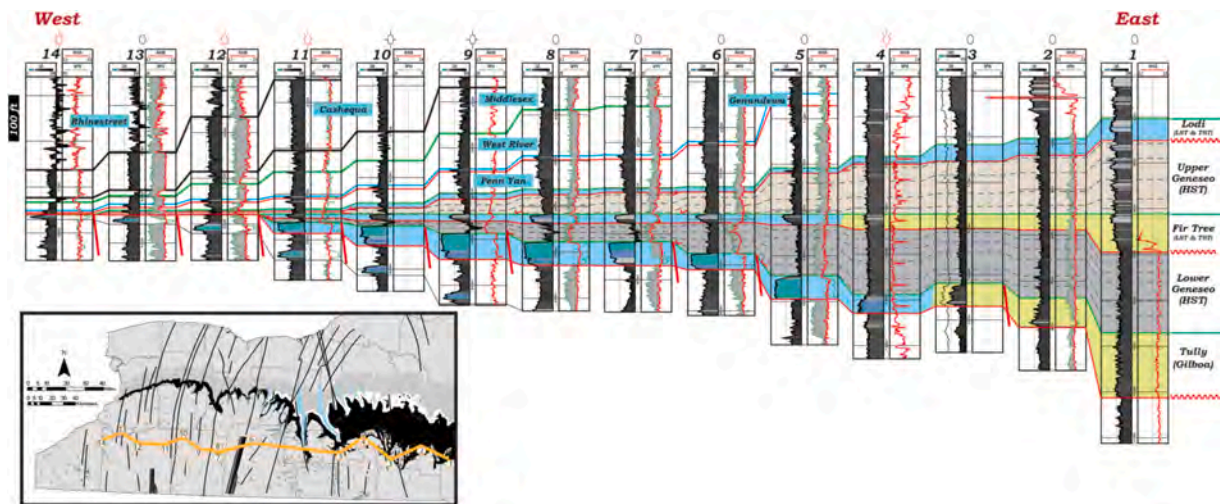
Fig. 22. East to west cross-section of the Hamilton Group through the Genesee Group. The underlying Tully/Gilboa interval increases in carbonate content to the west until it is completely truncated (*mfs* with erosion to west). The Lower Geneseo thins to the west with an increase in gamma-ray intensity (increasing organic-content to the west). Shows aggradational-progradational stacking patterns (HST) with downlap-onlap terminations on the underlying Tully (*mfs*). The Fir Tree interval increases in carbonate content to the west, and truncates the underlying Lower Geneseo. The Upper Geneseo thins to the west with an increase in gamma-ray intensity (increasing organic-content). Shows aggradational-progradational stacking patterns (HST) with downlap-onlap terminations on the underlying Fir Tree (*mfs*). Basement faults appear to strongly influence accommodation throughout the basin, particularly to the west where the Geneseo shows lapping onto the underlying Hamilton group.
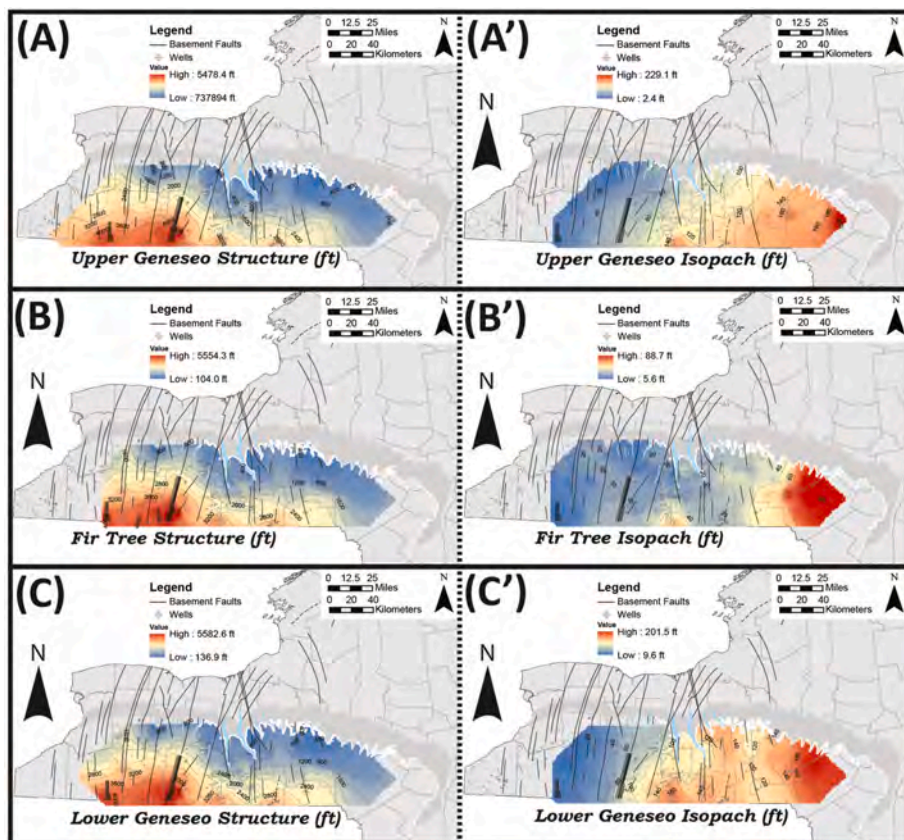
Fig. 23. Structure and isopach maps for the Geneseo Formation. (A) Upper Geneseo structure map and (A′) isopach map for the Upper Geneseo member representing a HST. Note the thickness variation associated with the N–S trending basement faults (black lines) reflecting organic-rich mud deposition filling in fractured basement topographic expression of the seafloor. (B) Fir Tree structure and (B′) isopach map representing the LST and TST. C) Lower Geneseo structure and (C′) isopach map representing a HST. The Lower Geneseo HST shows strong relationship between thickness variation and N–S trending basement structures. Preexisting basement structures created a fractured topographic expression of the seafloor. This accommodation was largely filled by the Lower Geneseo Member, and the Upper Geneseo HST shows a gradual thinning westward, indicating preexisting structure was relieved by the Lower Geneseo.

Geneseo show a gradual and sustained thinning to the west, indicating that the basement structures were no longer active in generating accommodation throughout the basin. Furthermore, this suggests that the previously generated accommodation had been filled in by the end of the Lower Geneseo HST, or, perhaps, by some of the Fir Tree (LST and TST). The Upper Geneseo is capped by a basin-scale unconformity (*sb*)

and transitions to overlying calcareous mudstones and limestones associated with the Lodi Limestone Member and associated units.

7. Unconventional reservoir characterization

Although the Geneseo Formation is termed a 'continuous shale gas
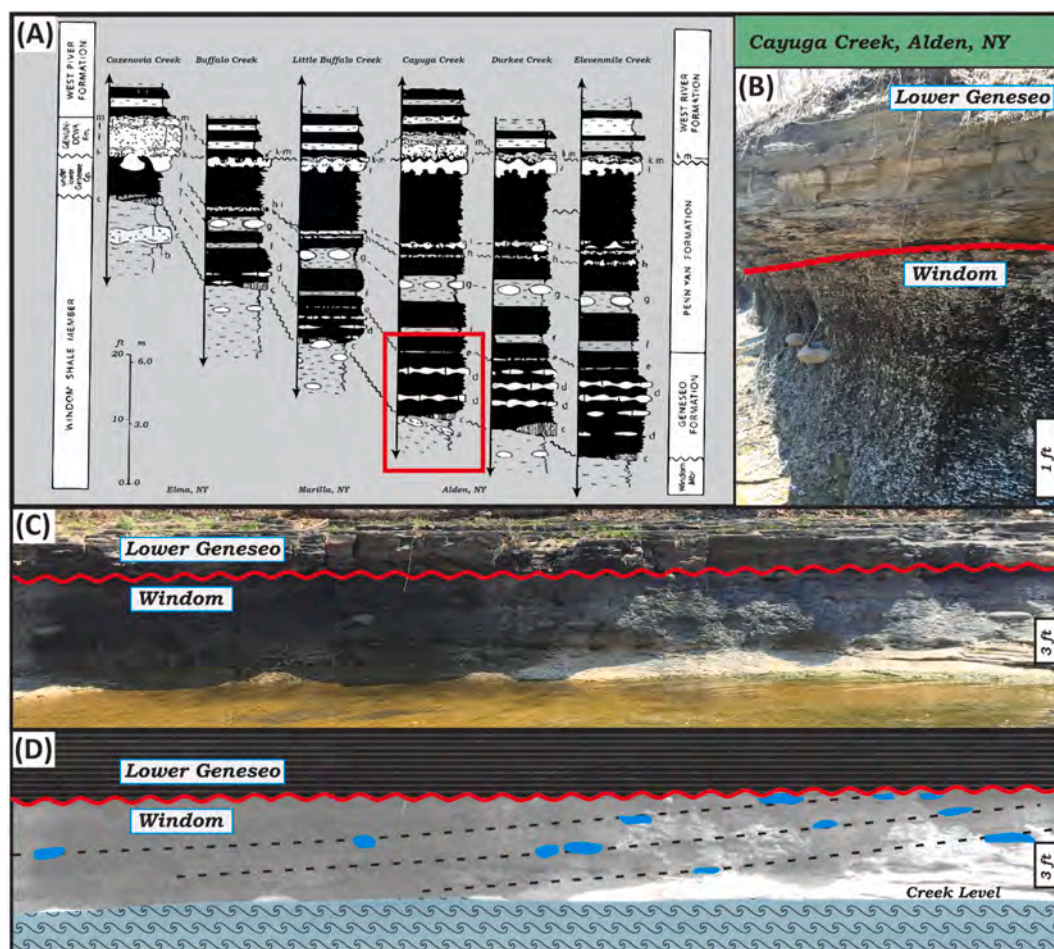
Fig. 24. A) Previous stratigraphic correlations in western New York of the Genesee Group, note Cayuga Creek where an angular unconformity was identified with the Geneseo and underlying Windom member (red box, Baird and Brett, 1991). B) Outcrop expression of angular unconformity between the Lower Geneseo HST and underlying Windom member of the Hamilton Group. This outcrop exposure is located in Cayuga Creek and is located along a N–S trending fault system. C) Overview image of Cayuga Creek exposure. D) Interpreted cross section highlighting unconformity (red line), bedding surfaces (black lines), and carbonate concretions (blue circles) along bedding planes highlighting the angular discordance. This outcrop is a key example of uplifted/down-dropped blocks associated with tectonism prior to lower Geneseo deposition similar to angular discordance observed in core (Fig. 7). (For interpretation of the references to colour in this figure legend, the reader is referred to the Web version of this article.)

accumulation' and prospective areas are widespread, understanding potential landing-zone variability is required for optimization. Such variability is controlled by facies, thickness, mechanical properties, organic-matter-richness, reservoir storage (Fig. 26), biogenic content, reservoir pressure, and other regional properties (Passey et al., 2010; Ottmann and Bohacs, 2014). Identifying optimal reservoir lithofacies within an unconventional play requires a thorough investigation of the distribution of hydrocarbon play elements within a predictive framework. For the Geneseo Formation, FA-1 and FA-2 are recognized to contain the optimal reservoir lithofacies due to:

- Elevated organic-matter content
- Abundance of OM and Mixed-system porosity
- Enrichment of silica cement
- Thinly-bedded with high vertical heterogeneity
- High lateral continuity

Radioactivity and formation-density logs are commonly used to identify zones of high TOC and gas potential for *in-situ* (self-sourced) unconventional plays (Passey et al., 2010). Since uranium adsorbs onto organic matter (Cumberland et al., 2016), abnormally high gamma ray and spectral gamma ray responses occur in zones of high TOC (Harper, 2008). Abnormally low formation density is observed in zones with high

TOC, which contain low-density organic matter along with free gas trapped in micropores and fractures and adsorbed gas trapped on organic macerals (Boyce and Carr, 2009). Cutoffs vary among operators, but intervals with GR > 140 API have been correlated with TOC >2 wt% in the Geneseo and Marcellus intervals (Smith and Leone, 2010). Using this relation, net ORP maps can be constructed for each interval in order to determine spatial distribution and thickness of optimal reservoir rock (Fig. 27). This mapping approach is conducted at the systems-tract scale which is considered to be the landing-zone scale (10's of feet) in these strata.

After these cutoffs are implemented at the systems-tract scale, the temporal distribution of optimal reservoir rock can be assessed within a chronostratigraphic framework (Fig. 27). For example, the Lower Geneseo HST shows 2 primary depocenters of optimal rock quality that are associated with basement structures and associated down-dropped structural elements that likely fostered increased accommodation growth. However, the Upper Geneseo HST records progradation of the system and a single depocenter for optimal rock quality develops westward from the underlying Lower Geneseo depocenters. If these cutoffs were applied to the entirety of the Geneseo Formation, the products would not be representative of the variance in reservoir quality observed at the systems-tract (landing-zone) scale. Furthermore, exploration efforts are significantly improved as the systems-tract scale
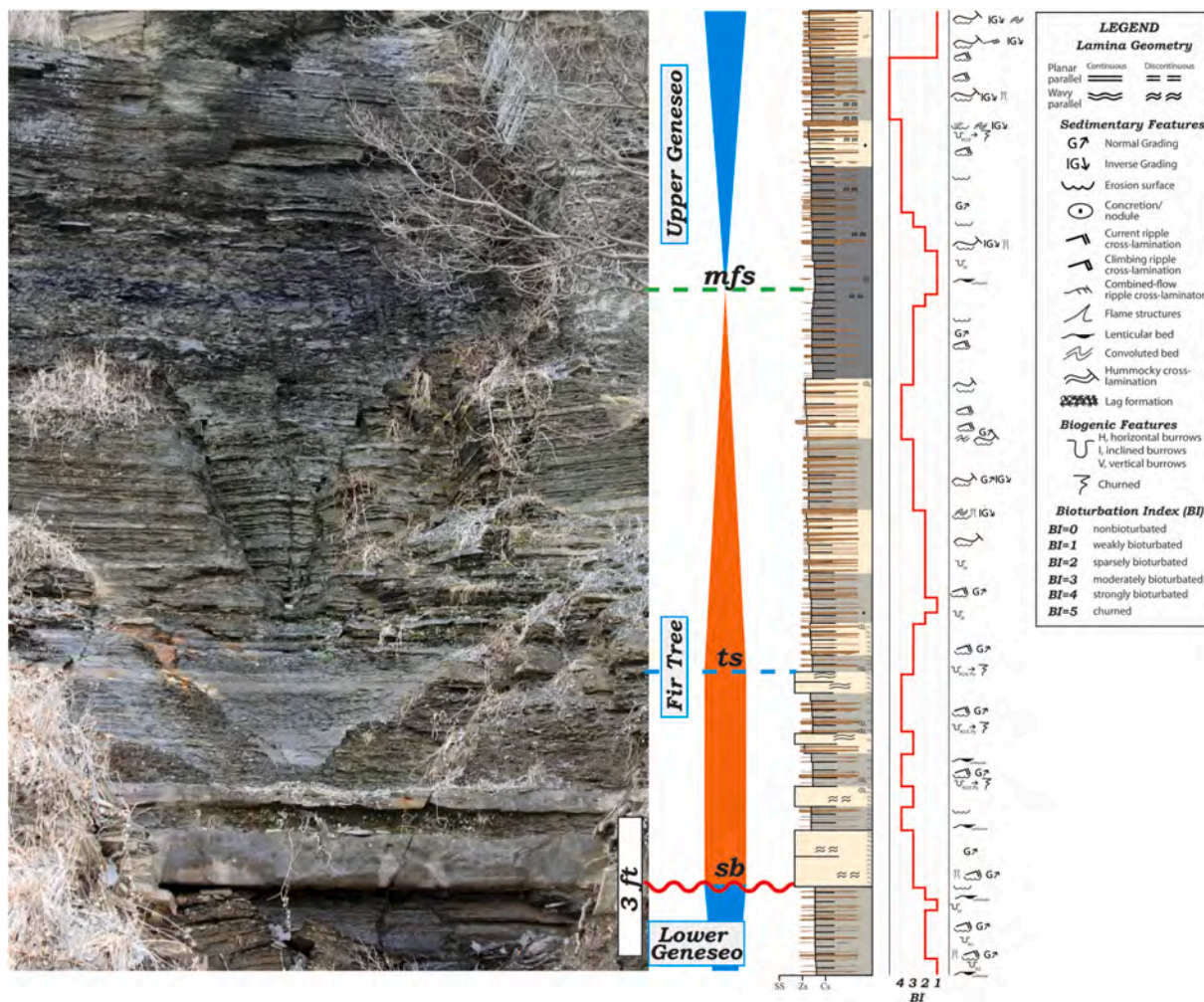
Fig. 25. Outcrop exposure of the Lower Geneseo sequence boundary, for the Fir Tree LST and TST overlying. Note the progradational-aggradational parasequence stacking patterns of the lower Fir Tree interval representing the LST, and the retrogradational stacking pattern in the upper Fir Tree interval representing the TST. A basin-scale *mfs* is identified at the base of the Upper Geneseo member and is easily identified in the sub-surface as a transition from low total gamma ray to high gamma ray response. Outcrops can provide regional context and stratigraphic architecture that is not captured in core or log data.

mapping reveals the stratigraphic complexity between the Lower Geneseo HST target and the Upper Geneseo HST target. Therefore, high-resolution geologic models are necessary to improve prediction capability at the landing-zone scale.

8. Discussion

Middle to Upper Devonian organic-matter-rich shales of the NAB are crucial secondary and tertiary targets to the extensively explored Marcellus sub-group. Although economic potential is recognized in these younger targets, prioritization of the Marcellus resulted in minimal data collection on "Upper Devonian" targets. Therefore, data on such key properties as organic-matter richness, composition, facies distribution, thickness variation, mechanical properties, and porosity have not been collected for these intervals in a predictive framework.

The Geneseo Formation has proven to be a key stratigraphic interval within the Appalachian basin due to the complex interaction between tectonic, depositional, and eustatic controls. Multiple unconformities have been identified in the Geneseo Formation, which can be mapped all across the Appalachian Basin into the Illinois Basin (Schieber and Lazar, 2004; Schieber and Wilson, 2013). A combination of observations suggest a broad depositional system throughout the Middle-Late Devonian of North America. For instance, unconformities are mapped to the western edge of the basin (and can be correlated to adjacent basins), the

lack of large-scale clinoforms in seismic data, and lack of deepwater (shoreline-detached) environments and depositional facies (e.g., basin floor fans, debris flows, slumps, etc.) which are necessary to produce the geometries and facies associations with the deepwater interpretation. There are numerous studies of deepwater systems (typically >200m water depth; Posamentier and Kolla, 2003), which have characteristic geometries, architectures, spatial dimensions, and depositional environments that are in every way inconsistent with the Devonian Appalachian Basin (shallow epicontinental seaway). For instance, deepwater systems originate with a submarine canyon (10's of kms wide) which is located on the slope and erosionally confined (V-shaped cross-section). Canyons are critical for sourcing sediment to the offshore deepwater setting through gravity-driven processes, with examples such as the Mississippi Canyon, Congo Canyon, and Monterey Canyon (Ferry et al., 2004; Goodwin and Prior, 1989; Maier et al., 2018). Canyons have also been identified in the Permian Basin which is also a deepwater depositional system (Zelt and Rossen, 1995; Beaubouef et al., 1999; Dutton et al., 2003; Wilson et al., 2020). Downdip, as the gradient of the slope weakens, sediment gravity flows are typically transported to a less deeply incised U-shape slope valley system (<10 km wide). As the gradient continues to reduce and the slope transitions to a basin floor setting, constructional channel-levee systems develop (in mud-rich systems; <5 kms wide) and transition to weakly confined channels (<10 kms wide) and unconfined distributary lobe deposits (10's of kms
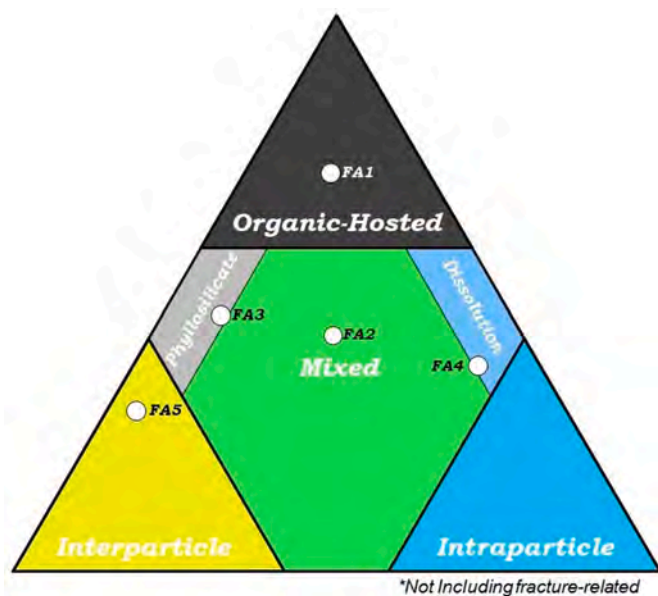
Fig. 26. Overview of reservoir storage and dominant pore system evolution within the Geneseo facies framework. Note this does not include fracture-related porosity.

Fig. 27. Net ORP maps for the Lower Geneseo (lower) and Upper Geneseo (upper) from gamma ray cutoffs (GR > 140) associated with TOC >2 wt%. Note the strong relationship with pay distribution and the N–S trending basement faults (black lines). The Lower Geneseo HST shows thick pay distribution in the south-central (blue arrows) associated with the convergence of basement faults and resulting down-dropped blocks that likely acted as sediment traps due to high accommodation generation, while western faults and associated uplifted blocks were likely topographic highs that acted as sediment baffles/barriers. There is a shift in depocenters between the Lower and Upper Geneseo ORP (blue arrows), indicating the Lower Geneseo healed much of the fractured topography and the basinward migration of the shoreline as the system progrades westward. The Clarendon-Linden fault system represents the western limit for the Geneseo. (For interpretation of the references to colour in this figure legend, the reader is referred to the Web version of this article.)

wide).

The aforementioned processes are driven by changes in local and regional gradient as well as sediment composition. Therefore, the products of these processes are predictable in nature, have key recognition criteria, as well as spatial relations that are inconsistent with the Devonian Appalachian basin. Because deepwater systems are detached from the shoreline, they are solely characterized by these environments and their respective gravity driven depositional processes. As mentioned in Smith et al. (2019), not one of these features have been identified in outcrops or subsurface datasets in the Appalachian basin. Rather, the organization and distribution of organic-rich shales in the Appalachian basin indicate a broad, shoreline-parallel depositional system. Additionally, the integration of subsurface datasets shows thickness trends that gradual thin basinward, rather than a fan or lobate morphology expected in a deepwater system. Additionally, the fact that deposits can be correlated for 100's of kilometers, as well as adjacent basins (i.e., Michigan and Illinois basins) is inconsistent with the spatial dimensions of any of the deepwater depositional processes which show strong heterogeneity (Conant and Swanson, 1961; Schieber and Lazar, 2004; Schieber and Wilson, 2013; Brett et al., 2018). Previous workers have also supported the notion that the Devonian Appalachian basin organic-rich shales were inconsistent with a shoreline-detached deepwater system (Conant and Swanson, 1961; Lundegard et al., 1985; Mccollum, 1988). However, the paradigm shift in mudstone sedimentology was necessary to provide the support for widespread deposition of fine-grained material through bedload processes (Schieber, 2009).

Recent sedimentologic studies have further provided the context to the dominant bedload transport of organic-rich muds in the Devonian Appalachian basin, including wave- and current-aided hyperpycnal flows which occur >100's of kms away from the shoreline (Wilson and Schieber, 2014; Lash, 2016). Furthermore, diminutive calcareous and agglutinated foraminifera reflecting shallow modern predominance facies suggesting inner neritic zone have been identified in these organic-matter-rich successions in western New York (Li et al., 2020). Dominant genera include several species of *Ammobaculites* and *Saccammina* which suggest that paleodepths did not exceed 50 m throughout the Frasnian (Li et al., 2020). These findings are aligned with the interpretation presented herein as the Geneseo lapped onto a series of positive structural elements westward in shallower water.

Therefore, this study further supports Smith et al. (2019) that all of these observations substantiate a shallow, broad depositional system attached to the shoreline which enables correlation across the entire basin, as well as adjacent basins during transgressions as the Cincinnati arch was inundated. In fact, there are examples along the Cincinnati arch where Middle-Late Devonian organic-matter-rich mudstones drape inside of karst features, suggesting multiple periods of exposure followed by inundation (Brett et al., 2004). Therefore, the organic-richness of Devonian Appalachian shales progressively increase to the west and is linked with distal, sediment starved settings, high primary productivity, under persistently dysoxic to intermittently anoxic conditions. Distal does not equal deep.

Recent recognition of hyperpycnites in this mudstone succession has revealed the dynamic modes of sediment transport in this organic-matter-rich mudstone succession (Wilson and Schieber, 2014). River-flood and storm-wave generated offshore directed underflows were responsible for transporting large volumes of fine-grained sediment and phytodetritus to offshore regions, and have been documented in the modern (Zavala et al., 2011, 2021; Zhang et al., 2018). The deposits of such flows can greatly impact reservoir quality in proximal-to

medial-shelf settings, due to rapid deposition of organic-matter-lean intervals dominated by clay- and silt-sized particles with terrestrial phytodetritus.

Scanning electron microscopy of the Geneseo Formation allowed definition of four principal pore types; (1) Phyllosilicate framework pores which are triangular openings (100–15000 nm wide) that are delineated by phyllosilicate frameworks, (2) organic-matter porosity (10–500 nm wide) found in kerogen macerals and organo-clay aggregates, (3) carbonate dissolution pores, and (4) interparticle pores. Therefore, porosity in the Geneseo is directly related to facies association accumulation within a sequence-stratigraphic framework, and corresponds to composition, texture, and organic-matter richness (Fig. 26).

The Lower Geneseo Member is an organic-matter-rich mudstone succession with aggradational to progradational parasequence stacking patterns (HST). Lower Geneseo laps down onto the underlying Tully Formation in central New York, and where the latter is absent in western New York, the Geneseo laps onto a significant unconformity marked by a pyritic-phosphatic lag that is interpreted as a *mfs*. The Fir Tree Member unconformably overlies the Lower Geneseo which shows toplap and truncation at this contact and displays progradational-aggradational-retrogradational parasequence stacking patterns (LST and TST), this interval is a regional biostratigraphic marker that separates the Lower and Upper Geneseo members (Baird et al., 1988; House and Kirchgasser, 1993). The Upper Geneseo Member is characterized by aggradational to progradational parasequence stacking patterns (HST), shows downlap-onlap stratal terminations with the underlying Fir Tree, and consists of dark gray silty mudstones and muddy siltstones with abundant current- and wave-formed features.

The Geneseo Formation shows characteristic stacking patterns in western New York that contradict previous interpretations that suggested that these deepwater, basinal black shales were continuously deposited from suspension settling. An alternative depositional model is proposed emphasizing the importance of bottom-current transport for delivering fine-grained clastics in a shallow (10's of meters water depth) epicontinental basin strongly influenced by basement structural

elements (Fig. 28). Additionally, this depositional model is consistent with the coarser-grained clastic facies from older and younger units in the Northern Appalachian basin (i.e., Ordovician Queenston Delta, Upper Devonian Canadaway Group Sandstones; Bird and Dewey, 1970; Bradley and Kidd, 1991; Smith and Jacobi, 2001). Thickness variation across the basin indicates that reactivation of basement structures strongly influenced accommodation (Figs. 23, 27 and 28). In particular, the N–S trending Clarendon-Linden Fault System resulting in fractured basinal topography associated with uplifted/down-dropped blocks that impact accommodation, with uplifted elements to the west acting as a western sediment barrier/baffle, particularly during lower Geneseo time. Therefore, as sediment was transported westward from the easterly source, it accumulated on a seafloor with substantial bathymetric relief due to fault reactivation during the third Tectophase of the Acadian orogeny (Ettensohn, 1987). Furthermore, the main depocenter was in south-central NY, where a structural low developed and trapped the fine-grained clastics of the Geneseo Formation. These complexities document the variability of rock properties in the Geneseo Formation, as well as structural control on sedimentation that can significantly change how landing zone variability is modeled.

9. Conclusions

- The Geneseo Formation can be subdivided into genetically related packages in the Appalachian Basin composed of 2 depositional sequences.
- Through developing a sequence stratigraphic framework, regional trends in rock properties can be mapped through detailed characterization of sedimentary environments.
- The Geneseo Formation is a key "Upper Devonian" target that requires an integrated sequence stratigraphic model to predict reservoir quality and distribution away from well control.
- Mudstone facies suggest a dynamic shelf environment with multiple modes of sediment transport and deposition. Facies associations are delineated into the following categories:
  1. Distal Organic-Matter-Rich Mudstones
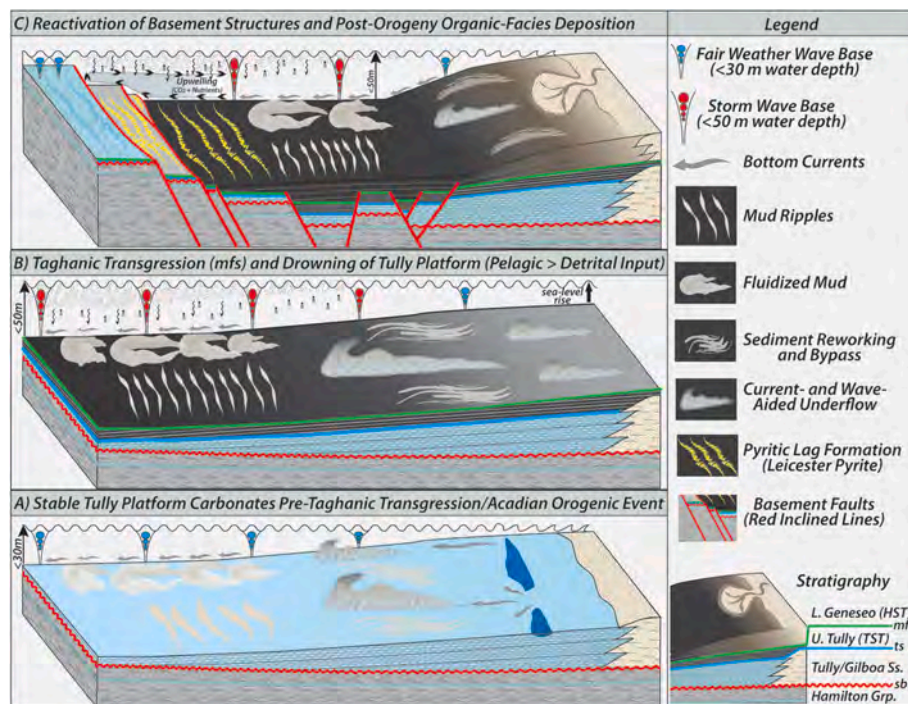
Fig. 28. East (right) to West (left) conceptual model in stratigraphic order for the evolution of the Tully to Geneseo Formation depositional setting and the transition from stable carbonate platform (A) to a drowned platform (B) and coupled thrust loading from the Acadian orogeny (east) and reactivation of basement structures (C) with interpreted sequence stratigraphic framework and depositional process.

2. Distal Organic-Matter-Rich Silty Mudstones and Argillaceous Siltstones
3. Medial Organic-Matter-Lean Silty Mudstones
4. Medial to Proximal Calcareous Silty and Sandy Mudstones
5. Medial to Proximal Argillaceous Siltstones and Sandstones

- Downlapping–onlapping stratal geometries show significant structural control on accommodation.
- Significant erosional bounding surfaces (unconformities) can be mapped and relate to structural flexing of the basin during Acadian Orogeny as well as eustatic change.
- Reservoir properties of the Marcellus may not be appropriate to apply to the Geneseo as an analog. Organic-matter-content, composition, porosity relations, and spatial distribution all show trends distinctly different from those in the Marcellus.
- Uplifted and down-dropped blocks associated with N–S basement faults formed a rugose seafloor which resulted in greater thickness of high TOC/GR facies or acted as sediment barriers/baffles to the west. Particularly in the Lower Geneseo, which should be considered in exploration and asset development.

Declaration of competing interest

Acknowledgements

References

Aboussalam, Z.S., 2003. Das Taghanic-Event im höheren Mittel-Devon von West-Europa und Marokko. Münstersche Forschungen zur Geologie und Paläontologie 97, 1–332.

Abreu, V., Neal, J.E., Bohacs, K.M., Kalbas, J.L., 2010. Sequence stratigraphy of siliciclastic systems—the ExxonMobil methodology atlas of exercises: SEPM (Society for Sedimentary Geology). Concepts Sedimentol. Paleontol. 9, 226.

Adams, J.A.S., Weaver, C.E., 1958. Thorium-to-uranium ratios as indicators of sedimentary processes—example of concept of geochemical facies. AAPG Bull. 42, 387–430.

Agbaji, A., Lee, B., Kuma, H., Belvalkar, R., Eslambolchi, S., Guiadem, S., Park, S., 2009. Sustainable Development and Design of Marcellus Shale Play in Susquehanna, PA, Report of EME580. Penn State University, State College, PA.

Algeo, T.J., Berner, R.A., Maynard, J.B., Scheckler, S.E., 1995. Late Devonian oceanic anoxic events and biotic crises: "rooted'' in the evolution of vascular land plants? GSA Today 5, 64–66.

Arthur, M.A., Dean, W.E., Pratt, L.M., 1988. Geochemical and climatic effects of increased marine organic carbon burial at the Cenomanian–Turonian boundary. Nature 335, 714–717.

Baird, G.C., Brett, C.E., 2008. Late Givetian Taghanic bioevents in New York state: new discoveries and questions. Bull. Geosci. 83, 357–370.

Baird, G.C., Brett, C.E., 1991. Submarine erosion on the anoxic sea floor: stratinomic, palaeoenvironmental, and temporal significance of reworked pyrite-bone deposits. In: Tyson, R.V., Pearson, T.H. (Eds.), Modern and Ancient Continental Shelf Anoxia, vol. 58. Geological Society of London, Special Publication, pp. 233–257.

Baird, G.C., Brett, C.E., Kirchgasser, W.T., 1988. Genesis and geochronology of black shale-roofed discontinuities in the Devonian Genesee Formation, western New York State. In: McMillan, N.J., Embry, A.F., Glass, D.J. (Eds.), Devonian of the World, vol. 14. Canadian Society of Petroleum Geologists Memoir, pp. 357–375.

Beaubouef, R.T., Rossen, C., Zelt, F.B., Sullivan, M.D., Mohrig, D.C., Jennette, D.C., 1999. Deep-water sandstones, Brushy canyon formation, west Texas. AAPG Contin. Educ. Course Note Ser. 40, 48.

Berner, R.A., 1990. Atmospheric carbon dioxide levels over Phanerozoic time. Science 249, 1382–1386.

Bhattacharya, J.P., MacEachern, J.A., 2009. Hyperpycnal rivers and prodeltaic shelves in the Cretaceous seaway of North America. J. Sediment. Res. 79, 184–209.

Bird, J.M., Dewey, J.F., 1970. Lithosphere plate-continental margin tectonics and the evolution of the Appalachian Orogen. Geol. Soc. Am. Bull. 81, 1031–1059.

Blakey, R., 2005. Paleogeography and Geologic Evolution of North America: Images that Track the Ancient Landscapes of North America.

Bohacs, K.M., Grawbowski, G.J., Carroll, A.R., Mankeiwitz, P.J., Miskell-Gerhardt, K.J., Schwalbach, J.R., Wegner, M.B., Simo, J.A., 2005. Production, destruction, and dilution – the many paths to source-rock development. In: Harris, N.B. (Ed.), The Deposition of Organic-Carbon-Rich Sediments; Models, Mechanisms, and Consequences, vol. 82. SEPM Special Publication, pp. 61–101.

Bohacs, K.M., Lazar, O.R., Demko, T.M., 2014. Parasequence types in shelfal mudstone strata– quantitative observations, lithofacies stacking patterns, and a conceptual link to modern depositional regimes. Geology 42, 131–134.

Bohacs, K.M., Norton, I.O., Gilbert, D., Neal, J.E., Kennedy, M., Borkowski, W., Rottman, M., Burke, T., 2012. The accumulation of organic-matter-rich rocks within an earth systems framework: the integrated roles of plate tectonics, atmosphere, ocean, and biota through the Phanerozoic. Principles Geol. Analysis 647–678.

Boyce, M.L., Carr, T.R., 2009. Lithostratigraphy and petrophysics of the Devonian Marcellus interval in West Virginia and southwestern Pennsylvania. In: Carr, T., gostino, D'AT., Ambrose, W., Pashin, J., Rosen, N.C. (Eds.), Unconventional Energy Resources: Making the Unconventional Conventional: 29th Annual GCSSEPM Foundation Bob. F. Perkins Research Conference, CD-ROM, pp. 254–281.

Boyer, D.L., Haddad, E.E., Seeger, E.S., 2014. The last gasp: trace fossils track deoxygenation leading into the Frasnian-Famennian extinction event. Palaios 29, 646–651.

Bradley, D.C., Kidd, W.S.F., 1991. Flexural extension of the upper continental crust in collisional foredeeps. Geol. Soc. Am. Bull. 103, 1416–1438.

Brett, C.E., Turner, A.H., McLaughlin, P.I., Over, D.J., Storrs, G.W., Baird, G.C., 2003. Middle–Upper Devonian (Givetian-Famennian) bone/conodont beds from central Kentucky, USA: reworking and event condensation in the distal Acadian foreland basin. Cour. Forschungsinst. Senckenberg 242, 125–139.

Brett, C.E., Baird, G.C., Bartholomew, A.J., 2004. Sequence stratigraphy of highly variable Middle Devonian strata in central Kentucky: implications for regional correlations and depositional environments. Annual Field Conference of the Great Lakes Section of SEPM 35–60.

Brett, C.E., Zambito, J.J., Baird, G.C., Aboussalam, S., Becker, T.R., Bartholomew, A.J., 2018. Litho-, bio-, and sequence stratigraphy of the Boyle-portwood succession (Middle Devonian, central Kentucky, USA). Palaeobiodivers. Palaeoenviron. 98, 331–368.

Bridge, J.S., Willis, B.J., 1991. Middle Devonian Near-Shore Marine, Coastal and Alluvial Deposits, Schoharie Valley, Central New York State, vol. 63. New York State Geological Association, Guidebook, pp. 131–160.

Bridge, J.S., Willis, B.J., 1994. Marine transgressions and regressions recorded in Middle Devonian shore-zone deposits of the Catskill clastic wedge. Geol. Soc. Am. Bull. 106, 1440–1458.

Chadwick, G.H., 1920. Large fault in western New York. Geol. Soc. Am. Bull. 31, 117–120.

Conant, L.C., Swanson, V.E., 1961. Chattanooga shale and related rocks of central Tennessee and nearby areas: U.S. Geological Survey Professional Paper 357, p. 91.

Cumberland, S.A., Douglas, G., Grice, K., Moreau, J.W., 2016. Uranium mobility in organic matter-rich sediments: a review of geological and geochemical processes. Earth Sci. Rev. 159, 160–185.

Dashtgard, S.E., Snedden, J.W., MacEachern, J.A., 2015. Unbioturbated sediments on a muddy shelf: Hypoxia or simply reduced oxygen saturation? Palaeogeogr. Palaeoclimatol. Palaeoecol. 425, 128–138.

Dashtgard, S.E., MacEachern, J.A., 2016. Unburrowed mudstones may record only slightly lowered oxygen conditions in warm, shallow basins. Geology 44, 371–374.

Donovan, A.D., Staerker, T.S., 2010. Sequence stratigraphy of the Eagle Ford (Boquillas) Formation in the subsurface of south Texas and outcrops of west Texas. Gulf Coast Assoc. Geol. Soc. Trans. 60, 861–899.

Dutton, S.P., Flanders, W.A., Barbon, M.D., 2003. Reservoir characterization of a permian deep-water sandstone, east Ford field, Delaware basin, Texas: American association of petroleum geologists. Bulletin 87, 609–627.

Ejofodomi, Efe, Baihly, Jason, Malpani, Raj, Altman, Raphael, Huchton, Terry, Welch, David, Zieche, J., 2011. Integrating All Available Data to Improve Production in the Marcellus Shale. North American Unconventional Gas Conference and Exhibition, The Woodlands, Texas, USA.

Ettensohn, F.R., 1985. In: Woodrow, D.L., Sevon, W.D. (Eds.), The Catskill Delta Complex and the Acadian Orogeny: a Model, vol. 201. Geological Society of America, Special Paper, pp. 39–49.

Ettensohn, F.R., 1987. Rates of relative plate motion during the Acadian Orogeny based on the spatial distribution of black shales. J. Geol. 95, 572–582.

Ferry, J.N., Babonneau, N., Mulder, T., Parize, O., Raillard, S., 2004. Morphogenesis of Congo submarine canyon and valley: implications about the theories of the canyons formation. Geodin. Acta 17, 241–251.

Formolo, M.J., Lyons, T.W., 2007. Accumulation and preservation of reworked marine pyrite beneath an oxygen rich Devonian atmosphere: constraints from sulfur isotopes and framboid textures. J. Sediment. Res. 77, 623–633.

Frakes, L.A., Francis, J.E., Syktus, J.I., 1992. Climate Modes of the Phanerozoic-The History of the Earth's Climate over the Past 600 Million Years. Cambridge University Press, Cambridge.

Gale, J.F.W., Laubach, S.E., Olson, J.E., 2014. Natural fractures in shale: a review and new observations. AAPG Bull. 98, 2165–2216.

Gingras, M.K., Bann, K.L., MacEachern, J.A., Waldron, J., Pemberton, S.G., 2009. A conceptual framework for the application of trace fossils. Appl. Ichnol. 52., 1–26.

Goodwin, R.H., Prior, D.B., 1989. Geometry and depositional sequences of the Mississippi canyon, Gulf of Mexico. J. Sediment. Petrol. 59, 318–329.

Grabau, A.W., 1913. Principles of Stratigraphy. Seiler, New York.

Hall, J., 1843. Geology of New York. Part IV, Comprising the Survey of the Fourth Geological District. Carrol & Cook, Albany, NY, p. 683p.

Harper, J.A., 2008. The Marcellus shale—an old "new" gas reservoir in Pennsylvania. Penn. Geol. 38, 2–13.

Harper, J.A., Abel, K.D., 1980. Net feet of radioactive shale in perrysburg Formation and Huron shale (Dunkirk facies), northwestern Pennsylvania: U.S. Department of energy, eastern gas shales Project. EGSP Series 25 scale 1:250,000.

House, M.R., Kirchgasser, W.T., 1993. Devonian goniatite Biostratigraphy and timing of facies movements in the Frasnian of eastern North America. In: Hailwood, E.A., Kidd, R.B. (Eds.), High Resolution Stratigraphy, vol. 70. Geological Society Special Publication, pp. 267–292.

Jacobi, R.D., Fountain, J.C., 2002. The character and reactivation history of the southern extension of the seismically active Clarendon– Linden Fault System, western New York State. Tectonophysics 353, 215–262.

Johnson, J.G., 1970. Taghanic onlap and the end of North American Devonian provinciality. Geol. Soc. Am. Bull. 81, 2077–2106.

Johnson, J.G., Klapper, G., Sandberg, C.A., 1985. Devonian eustatic fluctuations in Euramerica. Geol. Soc. Am. Bull. 96, 567–587.

Katz, B., Gao, L., Little, J., Zhao, Y.R., 2021. Geology still matters–Unconventional petroleum system disappointments and failures. Unconventional Res. 1, 18–38.

Kindle, E.M., 1896. The relation of the Ithaca group to the faunas of the portage and Chemung. Bull. Am. Paleontol. 2, 56.

Lash, G.G., 2016. Hyperpycnal transport of carbonaceous sediment — Example from the upper Devonian Rhinestreet shale, western New York, USA. Palaeogeogr. Palaeoclimatol. Palaeoecol. 459, 29–43.

Lazar, O.R., Bohacs, K.M., Macquaker, J.H.S., Schieber, J., Demko, T.M., 2015. Capturing key attributes of fine-grained sedimentary rocks in outcrops, cores, and thin sections: nomenclature and description guidelines. J. Sediment. Res. 85, 230–246.

Li, I., Bartlett, K., Kowalski, C., Bembia, P., Meehan, K.C., 2020. Paleoecology and predominance facies of Late Devonian Foraminifera in deltaic sequences of the Appalachian Basin, Western New York, U.S.A. J. Foraminifer. Res. 51, 32–45.

Lin, W., Bhattacharya, J.P., 2020. Depositional facies and the sequence stratigraphic control of a mixed-process influenced clastic wedge in the Cretaceous Western Interior Seaway: The Gallup System, New Mexico, USA. Sedimentology 67, 920–950.

Lundegard, P.D., Samuels, N.D., Pryor, W.D., 1985. Upper Devonian turbidite sequence, central and southern Appalachian basin: Contrasts with submarine fan deposits. In: Woodrow, D.L., Sevon, W.D. (Eds.), The Catskill Delta, vol. 201. Geological Society of America Special Paper, pp. 107–121.

MacEachern, J., Pemberton, S., 1992. Ichnological Aspects of Cretaceous Shoreface Successions and Shoreface Variability in the Western Interior Seaway of North America. SEPM Core Workshop. Soc. Econ. Paleontol. Mineral. 17, 57–84.

Maier, K.L., Johnson, S.Y., Hart, P., 2018. Controls on submarine canyon head evolution, migration, and fill in Monterey Bay, offshore central California. Mar. Geol. 404, 24–40.

Macquaker, J.H.S., Gawthorpe, R.L., Taylor, K.G., Oates, M.J., 1998. Heterogeneity, stacking patterns and sequence stratigraphic interpretation in distal mudstone successions: examples from the Kimmeridge Clay Formation, U.K. In: Schieber, J., Zimmerle, W., Sethi, P. (Eds.), Recent Progress in Shale Research. Schweizerbartísche Verlagsbuchhandlung, Stuttgart, pp. 163–186.

Mastalerz, M., Schieber, J., 2017. Effect of ion milling on the perceived maturity of shale samples: Implications for organic petrography and SEM analysis. Int. J. Coal Geol. 183, 110–119.

Maynard, J.B., 1981. Carbon isotopes as indicators of dispersal patterns in Devonian–Mississippian shales of the Appalachian Basin. Geology 9, 262–265.

Mccollum, L.B., 1988. A shallow epeiric sea interpretation for an offshore Middle Devonian black shale facies in eastern North America. In: McMillan, N.J., Embry, A.F., Glass, D.J. (Eds.), Devonian of the World, Volume II, vol. 14. Canadian Society of Petroleum Geologists, Memoir, Sedimentation, pp. 347–355.

Miller, K.B., Brett, C.E., Parsons, K.M., 1988. The paleoecologic significance of storm generated disturbance within a Middle Devonian muddy epeiric sea. Palaios 3, 35–52.

Neal, J., Abreu, V., 2009. Sequence stratigraphy hierarchy and the accommodation succession method. Geology 37, 779–782.

Ottmann, J., Bohacs, K., 2014. Conventional reservoirs hold keys to the 'Un's. AAPG Explor. 35, 26.

Passey, Q.R., Bohacs, K.M., Esch, W.L., Klimentidis, R., Sinha, S., 2010. From oil-prone source rock to gas-producing shale reservoir—Geologic and petrophysical characterization of unconventional shale–gas reservoirs. In: International Oil and Gas Conference and Exhibition. SPE Paper 131350, Beijing, China, p. 29. June 8–10, 2010.

Posamentier, H.W., Kolla, V., 2003. Seismic geomorphology and stratigraphy of depositional elements in deep-water settings. J. Sediment. Res. 73, 367–388.

Schieber, J., 1994. Evidence for high-energy events and shallow-water deposition in the Chattanooga Shale, Devonian, central Tennessee, USA. Sediment. Geol. 93, 193–208.

Schieber, J., 1998. Sedimentary features indicating erosion, condensation, and hiatuses in the Chattanooga Shale of central Tennessee: relevance for sedimentary and stratigraphic evolution: Stuttgart, E. Schweizerbart'sche Verlagsbuchhandlung Naegele u. Obermiller, Shales and Mudstones: I, Basin Studies. Sedimentol. paleontol. 187–215.

Schieber, J., 2009. Discovery of agglutinated benthic foraminifera in Devonian black shales and their relevance for the redox state of ancient seas. Palaeogeogr. Palaeoclimatol. Palaeoecol. 271, 292–300.

Schieber, J., 2011. Shale microfabrics and pore development – An overview with emphasis on the Importance of depositional processes. In: Leckie, D.A., Barclay, J.E. (Eds.), Gas Shale of the Horn River Basin. Canadian Society of Petroleum Geologists, Calgary, pp. 115–119.

Schieber, J., 2013. SEM Observations on Ion-milled Samples of Devonian Black Shales from Indiana and New York: The Petrographic Context of Multiple Pore Types. AAPG Memoir 102, 153–172.

Schieber, J., Lazar, R.O., 2004. Devonian Black Shales of the Eastern U.S.: New Insights into Sedimentology and Stratigraphy from the Subsurface and Outcrops in the Illinois and Appalachian Basins. Field Guide for the 2004 Great Lakes Section SEPM Annual Field Conference. Indiana Geological Survey Open File Study 90, 04-05.

Schieber, J., Wilson, R.D., 2013. Sedimentology and stratigraphy of shales: Expression and correlation of depositional sequences in the Devonian of Ohio and Kentucky. AAPG 2013 Annual Convention in Pittsburgh, Field Guide for Post-Convention Field Trip 9, 159.

Schieber, J., Lazar, R., Bohacs, K., Klimentidis, B., Ottmann, J., Dumitrescu, M., 2016. An SEM study of porosity in the Eagle Ford Shale of Texas – pore types and porosity distribution in a depositional and sequence stratigraphic context. AAPG Memoir 110, 153–172.

Schieber, J., Wilson, R.D., 2021. Burrows without a trace—How meioturbation affects rock fabrics and leaves a record of meiobenthos activity in shales and mudstones. PalZ 767–791.

Schmoker, J.W., 1981. Determination of organic-matter content of Appalachian Devonian shales from gamma-ray logs. AAPG Bull. 65, 1285–1298.

Smith, G.J., Jacobi, R.D., 2001. Tectonic and eustatic signals in the sequence stratigraphy of the Upper Devonian Canadaway Group, New York State. AAPG Bull. 85, 325–357.

Smith, L.B., Leone, J., 2010. Integrated Characterization of Utica and Marcellus Black Shale Gas Plays. AAPG Search and Discovery, New York State. Article #50289.

Smith, L.B., Schieber, J., Wilson, R.D., 2019. Shallow-water onlap model for the deposition of Devonian black shales in New York, USA. Geology 47, 279–283.

Thompson, J.B., Newton, C.R., 1987. Ecological reinterpretation of the dysaerobic Leiorhynchus Fauna: Upper Devonian Geneseo Black Shale, Central New York. Palaios 2, 274–281.

Ulrich, E.O., 1911. Revision of the Paleozoic systems. Geol. Soc. Am. Bull. 22, 281–680.

Van Tyne, A.M., 1975. Clarendon–Linden Structure, Western New York. New York State Geological Survey, Albany, Open file report.

Van Wagoner, J.C., Posamentier, H.W., Mitchum, R.M., Vail, P.R., Sarg, J.F., Loutit, T.S., Hardenbol, J., 1988. An overview of the fundamentals of sequence stratigraphy and key definitions. In: Wilgus, C.K., et al. (Eds.), Sea-Level Changes: an Integrated Approach, vol. 42. SEPM Special Publication, pp. 39–48.

Van Wagoner, J.C., Mitchum, R.M., Campion, K.M., Rahmanian, V.D., 1990. Siliciclastic sequence stratigraphy in well logs, cores, and outcrops. AAPG Methods in Exploration 7, 55.

Van Wagoner, J.C., Posamentier, H.W., Mitchum, R.M., Vail, P.R., Sarg, J.F., Loutit, T.S., Hardenbol, J., 1988. In: Wilgus, C.K., Posamentier, H., Roos, C.A., KendallSt, C. G.C. (Eds.), Sea-Level Changes – An Integrated Approach, 42. Society of Economic Paleontologists and Mineralogists Special Publication, pp. 39–45.

Venieri, M., Mackie, S.J., McKean, S.H., Vragov, V., Pedersen, P.K., Eaton, D.W., Galvis Portilla, H.A., Poirier, S., 2021. The Interplay between Cm- and M-Scale Geological and Geomechanical Heterogeneity in Organic-Rich Mudstones: Implications for Reservoir Characterization of Unconventional Shale Plays. Mar. Petrol. Geol. 132 (in press).

Weary, D.J., Ryder, R.T., Nyahay, Richard, 2000. Thermal maturity patterns (CAI and % R_o) in the Ordovician and Devonian rocks of the Appalachian basin in New York State: U.S. Geological Survey Open-File Report 496, 39.

Wilson, R.D., Schieber, J., 2014. Muddy Prodeltaic Hyperpycnites in the Lower Genesee Group of Central New York, USA: Implications For Mud Transport In Epicontinental Seas. J. Sediment. Res. 84, 866–874.

Wilson, R.D., Schieber, J., 2015. Sedimentary facies and depositional environment of the Middle Devonian Geneseo Formation of New York, U.S.A. J. Sediment. Res. 85, 1393–1415.

Wilson, R.D., Schieber, J., 2016. The Influence of Primary and Secondary Sedimentary Features on Reservoir Quality: Examples from the Geneseo Formation of New York, U.S.A. In: Olson, T. (Ed.), Imaging Unconventional Reservoir Pore Systems, vol. 112. AAPG Memoir, pp. 167–184.

Wilson, R.D., Schieber, J., 2017a. Sediment transport processes and lateral facies gradients across a muddy shelf: examples from the Geneseo Formation of central New York, United States. AAPG Bull. 101, 423–431.

Wilson, R.D., Schieber, J., 2017b. Association between wave- and current-aided hyperpycnites and flooding surfaces in shelfal mudstones: an integrated sedimentologic, sequence stratigraphic, and geochemical approach. J. Sediment. Res. 87, 1143–1155.

Wilson, R.D., Chitale, J., Huffman, K., Montgomery, P., Prochnow, S.J., 2020. Evaluating the depositional environment, lithofacies variation, and diagenetic processes of the Wolfcamp B and lower Spraberry intervals in the Midland Basin: Implications for reservoir quality and distribution. AAPG Bull. 104, 1287–1321.

Wilson, R.D., Schieber, J., Stewart, C.J., 2021. The discovery of widespread agrichnia traces in Devonian black shales of North America – Another chapter in the evolving understanding of a "not so anoxic" ancient sea. PalZ 95, 661–681.

Witzke, B.J., Heckel, P.H., 1988. Paleoclimatic indicators and inferred Devonian paleolatitudes of Euramerica. In: McMillan, N.J., Embry, A.F., Glass, D.J. (Eds.), Devonian of the World, vol. 14. Canadian Society of Petroleum Geologists, Memoir, pp. 49–63.

Woodrow, D.L., 1985. Paleogeography, paleoclimate, and sedimentary processes of the Late Devonian Catskill Delta. In: Woodrow, D.L., Sevon, W.D. (Eds.), The Catskill Delta, vol. 201. Geological Society of America, Special Paper, pp. 51–63.

Zambito, J.J., Brett, C., Baird, G.C., 2012. The late Middle Devonian (Givetian) global Taghanic biocrisis in its type area (Northern Appalachian Basin): geologically rapid faunal transitions driven by global and local environmental changes. In: Talent, J.A. (Ed.), Earth and Life: International Year of Planet Earth. Springer, pp. 677–703.

Zelt, F.B., Rossen, C., 1995. Geometry and continuity of deepwater sandstones and siltstones, Brushy Canyon Formation (Permian) Delaware Mountains, Texas. In: Pickering, K.T., Hiscott, R.N., Kenyon, N.H., Lucchi, F.R., Smith, R.D.A. (Eds.), Atlas of Deep Water Environments, Architectural Style in Turbidite Systems: London. Chapman and Hall, pp. 167–183.

Zavala, C., Arcuri, M., Gamero, H., Contreras, C., Meglio, M.D., 2011. A genetic facies tract for the analysis of sustained hyperpycnal flow deposits. In: Slatt, R.M., Zavala, C. (Eds.), Sediment Transfer from Shelf to Deep Water – Revisiting the Delivery System, vol. 61. AAPG Studies in Geology, pp. 31–51.

Zavala, C., Arcuri, M., Di Meglio, M., Zorzano, A., Otharan, G., Irastorza, A., Torresi, A., 2021. Deltas: A new classification expanding bates's concepts. J. Palaeogeogr. 10, 341–355.

Zhang, Y., Liu, Z., Zhao, Y., Colin, C., Zhang, X., Wang, M., 2018. Long-term in situ observations on typhoon-triggered turbidity currents in the deep sea. Geology 46, 675–678.

Zietz, I., 1982. Composite magnetic anomaly map of the United States; Part A, conterminous United States: US Geological Survey Geophysical Investigations Map GP-954-A, p. 59, 2 sheets, scale 1:2,500,000.